Event integration and temporal pattern separation: how hierarchical knowledge emerges in hippocampal subfields through learning.

Oded Bein[1] and Lila Davachi[2,3*]*

Affiliations

[1]Princeton Neuroscience Institute, Princeton University,
Princeton, NJ, 08540,

[2]Department of Psychology, Columbia University
New York, NY, 10027, United States

[3]Center for Clinical Research,
The Nathan S. Kline Institute for Psychiatric Research,
Orangeburg, NY, 10962, United States

*Correspondence: oded.bein@princeton.edu, ld24@columbia.edu

Key words

Hippocampus, event segmentation, CA3, dentate gyrus, pattern completion, pattern separation, attractor dynamics, high-resolution fMRI, encoding, learning

50 pages, 7 figures, 1 Supplementary Information.

Word count, abstract: 266

Word count, main text (excluding abstract, Methods and References): 7,769 (50,740 characters, including spaces)

Abstract

Everyday life experiences are composed of sequences of events determined by changes of contexts, layered with more rapidly changing occurrences that unfold within each event. A major challenge of our memory systems is how the brain integrates these occurrences within events while also maintaining their distinct details and avoiding over-integration across different contexts. Here we asked if and how distinct hippocampal subfields come to hierarchically represent both event context and subevents occurrences with learning. Participants learned repeating events, defined as sequences of objects superimposed on shared color frames, while undergoing high-resolution fMRI. Behavioral markers and consequences of event boundaries were evident across all repetitions. After learning, hippocampal CA3 multivoxel activation patterns reflected the event context and the strength of event representations in CA3 correlated with behavioral facilitation during event transitions. In contrast to CA3, dentate gyrus activation patterns became more differentiated through learning, specifically for objects that were close in time and belonged to the same event. This is a form temporal pattern separation that is sensitive to context, to facilitate distinct representations of subevent occurrences. A computational model explained these results by dynamic inhibition in dentate gyrus. We also adopted to fMRI novel similarity measures that are sensitive to the overlap in the population of activated voxels and show that CA3 representations of different contexts, and dentate gyrus' distinct item representations, likely result from different populations of voxels. These findings suggest an interplay between the representations of event context that shapes temporal pattern separation in dentate gyrus, and attractor dynamics in CA3. The results advance our knowledge of how the hippocampus represents context and time.

Introduction

A challenge to a memory system is how to distinguish similar experiences that occur in the same context to avoid confusion, while also generalizing across these same experiences to extract shared context-relevant knowledge. Changes of context, termed event boundaries, are essential to constructing context-relevant knowledge because they cause us to parse continuous experience into discrete episodes, or events (Bird, 2020; Clewett et al., 2019; Clewett & Davachi, 2017; Maurer & Nadel, 2021; Radvansky & Zacks, 2017; Zacks, 2020; Zacks et al., 2007). These events unfold in time and within each event, layered on a stable context, there is a higher frequency sequence of occurrences or subevents. For example, making breakfast entails of a sequence of subevents such as brewing coffee and frying eggs, and is a distinct event from leaving our house to commute to work. As events become more familiar, such as our everyday-life routines, learning provides opportunity to integrate subevents belonging to the same event, which can improve linking information in memory (DuBrow & Davachi, 2014; Ezzyat & Davachi, 2014; Paz et al., 2010). However, integration can also blur the distinction of event details, as well as confuse the representations of different events and lead to interference in memory (e.g., Brown & Stern, 2013; Chanales et al., 2019; Favila et al., 2016; Wanjia et al., 2021). How do we integrate only the information belonging to the same context, or event, without linking irrelevant information from different events? And, how does our brain integrate information in the same context while also maintaining detailed representations of subevents?

Computations supported by distinct hippocampal subfields might help to solve these challenges (Norman & O′Reilly, 2003; O′Reilly & McClelland, 1994; Treves & Rolls, 1994; Yassa & Stark, 2011). Across humans and animal models, the hippocampus has been implicated in the representation of context, time, and sequential events (Bellmund et al., 2020; Brown et al., 2014;

Buzsáki & Tingley, 2018; Davachi & DuBrow, 2015; Deuker et al., 2016; Eichenbaum, 2017; Heusser et al., 2016; Liu et al., 2022; O′Keefe & Dostrovsky, 1971; O′Keefe & Nadel, 1978; Pastalkova et al., 2008; Paz et al., 2010; Ranganath & Hsieh, 2016; Schendan et al., 2003; Thavabalasingam et al., 2019; Umbach et al., 2020; J. Zheng et al., 2022). Importantly, the hippocampus is also known to represent task elements (Aly & Turk-Browne, 2016a, 2016b; Chung et al., 2021; Mızrak et al., 2021; Tambini & Davachi, 2013). In humans, we can closely control, through instruction, participants attention to the context of an event as well as items in that context and their temporal position. We leveraged this ability to ask whether and how hippocampal subregions hierarchically represent events and their subevents (McKenzie et al., 2014). We focused on CA3 and dentate gyrus (DG) that are thought to create integrated vs. distinct representations (Hainmueller & Bartos, 2020; Hasselmo & Eichenbaum, 2005; Horner & Doeller, 2017; Kesner, 2018; Knierim & Neunuebel, 2016; Marr, 1971; Nakazawa, 2017; O′Reilly & McClelland, 1994; Treves & Rolls, 1994; Yassa & Stark, 2011). Specifically, we asked whether CA3 integrates information based on context, while DG distinctly represents subevents to maintain specific details.

The highly interconnected auto-associative networks within CA3 have been hypothesized to promote attractor dynamics (Kesner & Rolls, 2015; Knierim & Neunuebel, 2016; Treves & Rolls, 1994), which might contribute to integrating event representations. Models of CA3 that use attractor dynamics propose that similar neural representations inputted to CA3 converge to the same CA3 activity pattern, a process known as pattern completion, whereas different inputs are attracted towards different activity patterns in CA3 (Knierim & Neunuebel, 2016; Lee et al., 2004; Marr, 1971; Rolls, 2016; Treves & Rolls, 1994; Vazdarjanova & Guzowski, 2004; Yassa & Stark, 2011). Across subevents that unfold in the same higher-level event, the auto-associative network

in CA3 can lead to the persistence of activity patterns that maintain a stable context representation and results in similar representations within the same event (Hasselmo & Eichenbaum, 2005; Howard et al., 2005; Howard & Kahana, 2002; Hsieh et al., 2014; Kesner & Rolls, 2015; Levy, 1996; Polyn et al., 2009). At event boundaries, the changing perceptual input drives CA3 representations towards a different activity pattern representing the new context (Hasselmo & Eichenbaum, 2005; Kesner & Rolls, 2015). Thus, we propose that contextual stability within the same event together with a shift to a different activity pattern between events can be a mechanism by which attractor dynamics lead to event representations in CA3 (Clewett et al., 2019; Davachi & DuBrow, 2015; Horner et al., 2015; Horner & Burgess, 2014; Liu et al., 2022). Indeed, our prior work has shown that stability of hippocampal representations correlates with temporal memory for event sequences (DuBrow & Davachi, 2014; Ezzyat & Davachi, 2014). Consistent with this, it has been shown during retrieval that the magnitude of activation in CA3 is related to the holistic retrieval of events (Grande et al., 2019; Horner et al., 2015). Thus, we hypothesized that CA3 will integrate representations of information occurring within the same event while separating across different events.

As attractor dynamics in CA3 may pull the representations of items from the same event into a more similar space, a complementary mechanism is needed to distinguish these same sequential representations, to allow knowledge of event details. The DG has long been implicated in a process called pattern separation, whereby distinct neural representations are allocated to highly similar inputs (Baker et al., 2016; Bakker et al., 2008; Berron et al., 2016; Brown et al., 2014; Danielson et al., 2016; Kirwan & Stark, 2007; Lacy et al., 2011; J. K. Leutgeb et al., 2007; S. Leutgeb & Leutgeb, 2007; Nakazawa, 2017; Neunuebel & Knierim, 2014; Newman & Hasselmo, 2014; O′Reilly & McClelland, 1994; Treves & Rolls, 1994; Wanjia et al., 2021). Thus,

we designed this study to assess whether DG processing also contributes to *temporal pattern separation*. In rodents, DG lesions impair temporal memory (Morris et al., 2013) and, in humans, a prior study showed increased fMRI BOLD signal in CA3/DG in response to changes in the order of sequences of items (Azab et al., 2014), suggesting sensitivity to temporal order. However, this study reported average BOLD signal, and thus did not directly measure the neural representations in DG. Interestingly, a recent in-vitro study found that temporally similar spike trains inputted to DG tissue resulted in divergent DG activity patterns, providing some initial evidence for pattern separation in time (Madar et al., 2019). However, whether DG performs temporal pattern separation as events unfold in time, and whether changes of context modulate temporal pattern separation, is unknown.

We hypothesized that during learning of repeating sequential events, CA3 attractor dynamics may integrate information within event, while keeping the representations of different events distinct. By contrast, DG separation may be especially important within the same event. DG may pattern separate specifically experiences that share the same context and are close in time, and therefor are temporally and perceptually most similar. To test these hypotheses, we repeatedly exposed participants to temporally extended events of sequentially presented objects. Objects were embedded in colored frames that served as a shared context, switching every four objects to create different events (Heusser et al., 2016, 2018). In behavior, both reaction times during learning events and later memory demonstrate that participants segment well-learned events. We used high-resolution fMRI to dissociate DG and CA3 in humans and tracked multivoxel activity patterns in CA3 and DG during learning events. Briefly, in CA3 learning led to higher pattern similarity between objects in the same event compared to across events, irrespective of the temporal distance between items, suggesting integration within events and separation between events. Event

representations in CA3 also correlated with a behavioral facilitation of transitioning between events, as measured by reaction times during event transitions. By contrast, DG representations after learning differentiate objects that are close, but not far apart, in time, specifically when these objects appear in the same context, and therefore belonged to the same event. This result might reflect temporal pattern separation in DG that is sensitive to context shifts. We then propose a dynamic inhibition model that might yield such an effect and substantiate this hypothesis using simulations. We additionally adopted to human fMRI novel similarity measures previously used in rodents (Madar et al., 2019), to gain further support for the notion that different populations of voxels are involved in representing different items (in DG) or events (in CA3), consistent with attractor dynamics in CA3 and the proposed dynamic inhibition model in DG. Together, these results advance our knowledge of how hippocampal representations structure time and context during learning. They demonstrate how our brain might build hierarchically structured knowledge through integration and separation at different levels of event representations.

Results

Behavioral measures of learning

Participants were exposed to repeating sequences of objects superimposed on a colored frame and were asked to make judgments about the pleasantness of the object-color combination for each object. The color of the frame changed every 4 objects, representing a change in context that was operationalized as an event boundary (Figure 1A; Heusser et al., 2016, 2018). Previous studies have shown that, for once-presented events, processing time increases at event boundaries, reflecting a cost to transitioning to a new event (Heusser et al., 2018; Pettijohn & Radvansky, 2016; Zwaan, 1996). We investigated whether this marker of event segmentation persists with

repetitions, indicating that participants continue to segment repeated events. Single-trial RTs for the pleasantness judgments were entered into mixed-level general linear models (Lo & Andrews, 2015), testing the effects of Boundary, Repetition, and their interaction. These models revealed a strong effect of Repetition, reflecting that participants got significantly faster over repetitions (Figure 1B), indicating learning ($\chi^2_{(1)} = 3499.4$, $p < .0001$, AIC reduction: 3497). We also found a main effect of Boundary ($\chi^2_{(1)} = 373.87$, $p < .0001$, AIC reduction: 372), indicating slower RTs for boundary compared to non-boundary items. We found no interaction of Repetition by Boundary ($\chi^2_{(1)} = 0.02$, $p = .89$). These results suggest that slower RTs at the boundary persisted through repetitions, as events become well learned (Figure 1B). To further demonstrate the persistence of slow RTs at the boundary across repetitions, we tested each repetition separately, and found a strong effect of Boundary in each repetition ($\chi^2_{(1)}$'s > 86, p's < .0001, AIC reductions > 74). Thus, boundaries influence RTs for novel as well as familiar and well learned events (Zwaan et al., 1995).

After the learning of each list, we tested temporal memory for adjacent items from the list using a serial recognition memory test. In each trial, participants were cued with an object from the list and asked to select from two options the object that came next in the list (Figure 1C). We tested temporal memory for three types of pairs: Pos1-2, Pos2-3 and Pos4-1 (the first number represent the event position of the cue, and second number the event position of the target). As expected from presenting the sequences over 5 repetitions during learning, participants were highly accurate and confident in their responses, indicating that the lists were well learned (Accuracy: Pos1-2: $M = 88.24$, $SD = 11.91$, Pos2-3: $M = 88.24$, $SD = 10.33$, Pos4-1: $M = 88.33$, $SD = 10.74$; High-confidence hits: Pos1-2: $M = 81.20$, $SD = 18.35$, Pos2-3: $M = 80.96$, $SD = 18.20$, Pos4-1: $M = 88.33$, $SD = 18.60$, rate calculated out of total responses). No difference was observed in

accuracy or high-confidence rates for the three memory trials (One-way repeated measures ANOVA with the factor of Event Position: Accuracy: $F_{(2,58)} = .003$, $p = .997$; High-confidence: $F_{(2,58)} = .39$, $p = .68$).

The event structure of the task was evident in participants RTs during retrieval (Radvansky & Zacks, 2017; Swallow et al., 2009). Interestingly, RTs were significantly slower for Pos4-1 trials, when participants had to make a temporal memory judgement for items that were from adjacent events, compared to those drawn from the same event (Pos1-2, Pos2-3; Figure 1C). Single-trial RTs were entered to a mixed-level general linear model (Lo & Andrews, 2015), which revealed a strong effect of Event Position (Pos1-2/Pos2-3/Pos4-1; $\chi^2_{(2)} = 30.23$, $p < .0001$, AIC reduction: 26.23). Planned pairwise comparisons between specific pairs of positions revealed that RTs in Pos4-1 were slower compared to both Pos1-2 and Pos2-3 (Pos4-1 vs. Pos1-2: $\chi^2_{(1)} = 31.40$, $p < .0001$, AIC reduction: 29.41; Pos4-1 vs. Pos2-3: $\chi^2_{(1)} = 6.12$, $p = .013$, AIC reduction: 4.12). This result indicates that the temporal order of memories that bridged an event boundary was less accessible to our participants. This is consistent with previous studies with once-presented events (DuBrow & Davachi, 2013, 2014; Ezzyat & Davachi, 2011, 2014), but extends that work to show that repeated events are still segmented in memory. We also found that RTs for Pos2-3 were longer compared to Pos1-2 ($\chi^2_{(1)} = 10.42$, $p = .0012$, AIC reduction: 8.42), suggesting better memory when memories are cued with a boundary item, consistent with prior work (Heusser et al., 2018; Swallow et al., 2009). Together, the behavioral results during list learning and in the following temporal memory test indicate that events were segmented (Hard et al., 2006; Zwaan et al., 1995).

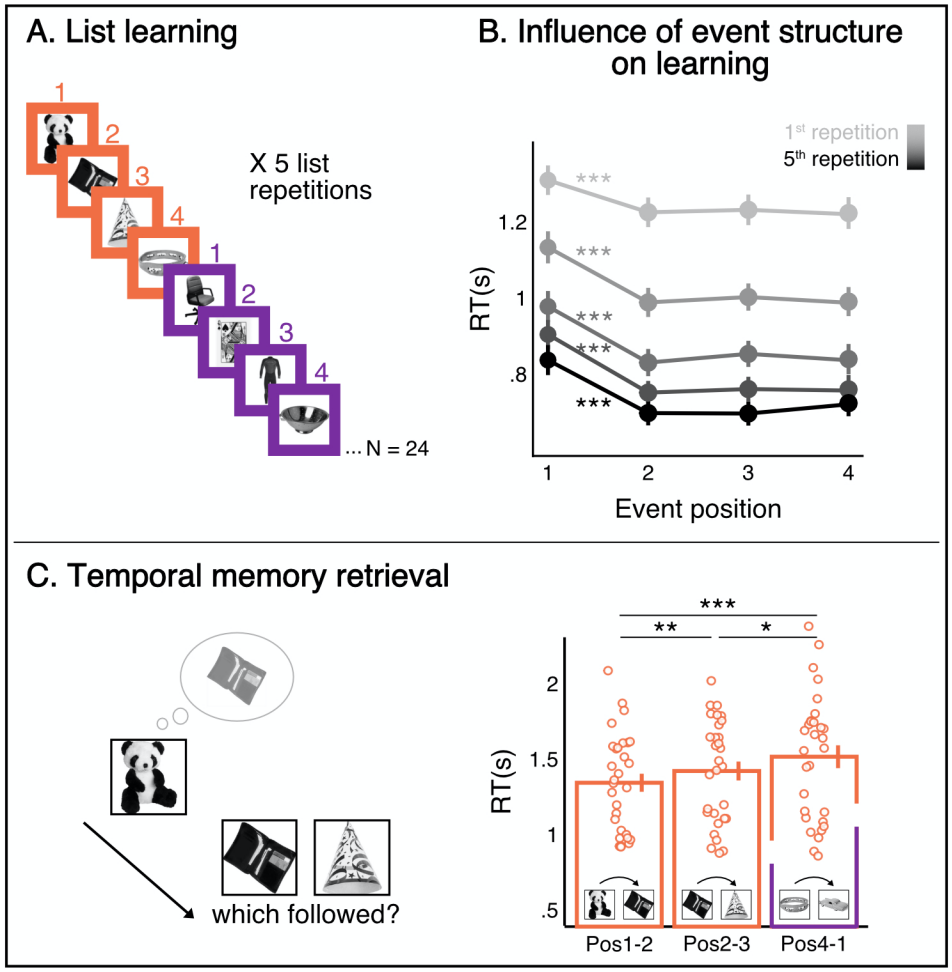

Figure 1. Paradigm and behavior: event structure is evident in behavior. A. During list learning, participants observed lists of 24 objects on colored frames. The color frame changed every 4 objects, creating distinct events. Each list repeated 5 times. B. Reaction times (RT) during list learning showing higher RT for boundary items, a marker of event segmentation, persisting through the 5th repetition. C. Left: at the end of the 5 repetitions of each list, we tested temporal order memory, by showing a cue from the list, prompting participants to retrieve the following item from the list, and then choose the correct item. Right: RT in the temporal memory test are presented for all trial types. N = 30. Data are presented as mean values, error bars reflect +/- SEM. * p = .01, ** p = .001, *** p < .0001. Statistical analysis was conducted by entering single trial RTs to general linear mixed-effects models and conducting model comparisons using Chi-square tests.

Univariate activation decreases with learning in DG, but not in CA3

To establish that CA3 and DG can be dissociated in human fMRI, we first examined univariate activation (average fMRI BOLD response) in DG and CA3 over the course of learning. To this end, the univariate activation estimates during learning (t-statistics resulting from a standard GLM

analysis, see Methods) per each event position and repetition and per each participant, averaged across all voxels in each ROI, were entered to a repeated measures ANOVA with the factors of Event Position (1 through 4), Repetition (Rep1/Rep5), ROI (CA3/DG), and Hemisphere (right/left). We found a main effect of ROI ($F_{(1,29)} = 7.69$, $p = .0096$, $\eta_p^2 = .21$), indicating that univariate activation differed between CA3 and DG. We also found an interaction of Repetition by ROI ($F_{(1,29)} = 8.013$, $p = .008$, $\eta_p^2 = .22$), demonstrating that repetition differentially modulated activity in CA3 vs. DG. A marginal effect of Event Position by Hemisphere was also observed ($F_{(1,29)} = 2.99$, $p = .094$, $\eta_p^2 = .09$); all other effects were not significant (F's$_{(1,29)} < 2.36$, p's $> .13$).

We followed up on the ROI by Repetition interaction by testing the effect of Repetition within each ROI, collapsed across hemispheres. Activation levels in each ROI were entered to a repeated measures ANOVA with Event Position and Repetition. We found a significant main effect of Repetition in DG ($F_{(1,29)} = 5.577$, $p = .025$, $\eta_p^2 = .16$), but not in CA3 ($F_{(1,29)} = .34$, $p = .56$). No effects of Event Position nor an interaction were observed (F's$_{(1,29)} < 2.20$, $p > .14$). These results reflect a decrease in univariate activation in DG from the 1st repetition to the 5th repetition, while CA3 activation levels remained similar, and even numerically increased (DG: Rep1: $M = .082$, $SD = .15$, Rep5: $M = .001$, $SD = .17$; CA3: Rep1: $M = .006$, $SD = .13$, Rep5: $M = .027$, $SD = .16$; average across Event Positions, see Supplementary Figure 1). Thus, in our data, CA3 vs. DG revealed different activation profiles.

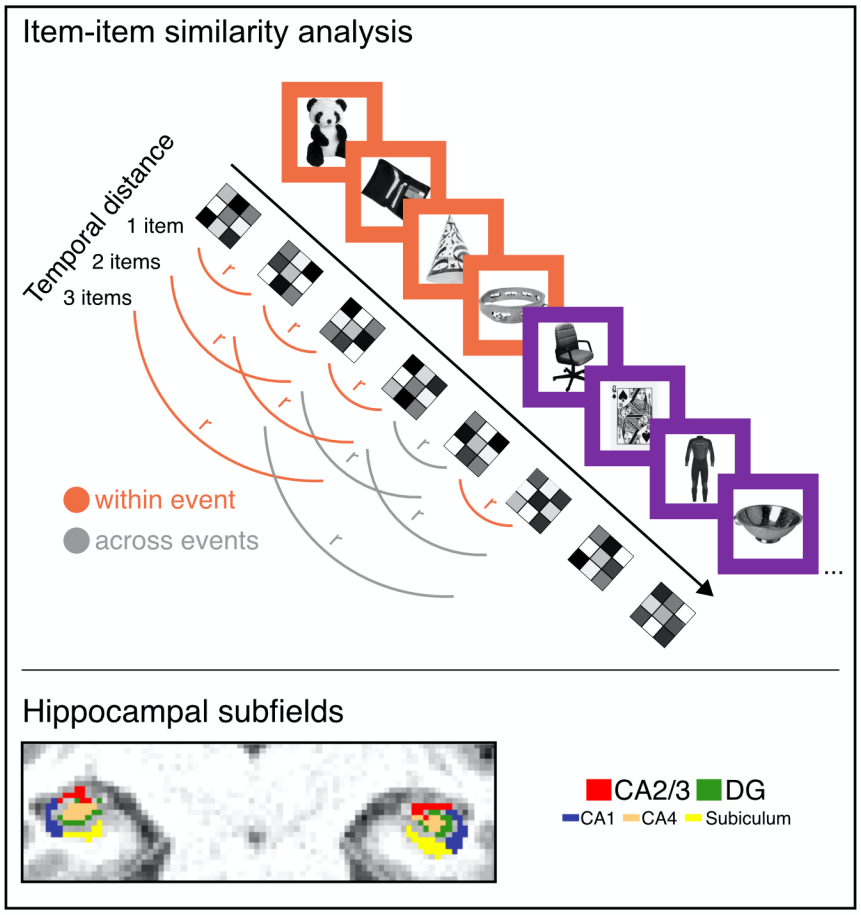

Figure 2. Item-item similarity in hippocampal subfields based on context and time. Top: we extracted the multivoxel activity patterns per item in the list, and computed similarity between items that belonged to the same event (within event similarity) versus items that belonged to different events (across events similarity). We also computed similarity for items that were with temporal distance of 1 item as well as temporal distance of 2 or 3 items. Bottom: patterns were extracted in hippocampal subfields, that were automatically segmented. The image shows segmentation in one participant's anatomical space.

Different event representations in the left CA3 versus DG

To test our main questions regarding neural representations in CA3 and DG, we computed the similarity between multivoxel activity patterns corresponding to sequential objects across learning repetitions (Figure 2). To specifically target changes in multivariate patterns specifically corresponding to the learning of event structure, we used the first presentation of each list as a baseline and subtracted the similarity values for the first presentation from those measured during all subsequent presentations (Schapiro et al., 2012; Schlichting et al., 2015). This allowed us to specifically target learning-related changes in pattern similarity while controlling for correlations that might stem from the BOLD signal characteristics and analysis steps, which are identical in all repetitions (Mumford et al., 2014; Schapiro et al., 2012; Schlichting et al., 2015); Methods).

Similarity values were computed for three different temporal distances (lag 1,2, and 3 items), i.e., similarity between an object and the immediately following object (lag 1), or the object presented two or three trials later, with lag 3 being the maximum temporal distance within an event. These similarity values between objects that appeared in the same event (within event) could therefore be compared to similarity values between objects with the same temporal distance, but from different events (across events; Figure 2, Methods). The similarity values per pair of objects were entered to a mixed-effects linear model that examined the interaction between Event (within event/across events), ROI (CA3/DG), and Hemisphere (right/left). Hemispheres were treated separately due to previously reported lateralized representational similarity effects in hippocampal subfields (Bein et al., 2020; Dimsdale-Zucker et al., 2018; Kim et al., 2017; Kyle, Stokes, et al., 2015; Schlichting et al., 2015; Stokes et al., 2015) as well as in hippocampal event representations (DuBrow & Davachi, 2013; Ezzyat & Davachi, 2014; Heusser et al., 2016; Hsieh et al., 2014). The three-way interaction between Event, ROI and Hemisphere was significant ($\chi^2_{(1)} = 12.91$, $p = .0003$, AIC reduction: 10.91), demonstrating different event representations in CA3 vs. DG that were also modulated by hemisphere. Thus, we followed up and examined the interaction of Event by ROI within each hemisphere. This analysis revealed a strong interaction of Event by ROI in the left hemisphere ($\chi^2_{(1)} = 19.27$, $p = .00001$, AIC reduction: 17.27), but not in the right hemisphere ($\chi^2_{(1)} = .43$, $p = .51$). Therefore, further analyses were limited to the left hemisphere. Left CA3 and DG similarity values are presented in Figures 3 and 6, where we focused on the 5th repetition (see below; for all repetitions, see Supplementary Figure 2).

Event representations in the left CA3

To further characterize the nature of the differences between CA3 and DG, we first focused on the left CA3. Pattern similarity values for objects with all temporal distances (lag 1, 2, 3), within and across events, were entered to mixed-level models testing the effect of Event (within/across), Temporal Distance (lag 1, 2, 3), as well as their interaction (first irrespective of repetition). In CA3, we found a main effect of Event (within vs. across: $\chi^2_{(1)} = 9.06$, $p = .0026$, AIC reduction: 7.06; Figure 3 and Supplementary Figure 2), with higher similarity values within, compared to across events. Including Repetition (1-5) in the model yielded a marginally significant interaction of Event by Repetition ($\chi^2_{(1)} = 3.61$, $p = .057$; AIC reduction: 1.61). There was no main effect of Temporal Distance ($\chi^2_{(1)} = 2.22$, $p = .13$), nor interaction effects for Event by Temporal Distance ($\chi^2_{(1)} = .04$, $p = .84$) or of Event by Temporal Distance by Repetition ($\chi^2_{(1)} = .01$, $p = .92$). Thus, these results revealed that CA3 representations are significantly more similar within versus across adjacent events, irrespective of the temporal distance of the measured items. Therefore, CA3 develops representations of sequential events. We next examined the 2nd and 5th repetitions separately, to target patterns early versus late in learning. No main effect of Event was found in the 2nd repetition ($\chi^2_{(1)} = 1.55$, $p = .21$). By the 5th repetition, however, when events were well learned, within event similarity was significantly higher compared to across event similarity ($\chi^2_{(1)} = 5.42$, $p = .02$, AIC reduction: 3.42, Figure 3), showing that CA3 event representations were refined by learning. Importantly, the results remained the same when accounting for univariate activation (Supplementary Information). Although not the aim of the current study, when examining similarity values for different event positions (1-4), similarity with the beginning and ending of an event were numerically higher than similarity with the middle of an event (Supplementary Figure 3, see Discussion). Additionally, a control analysis confirmed that CA3

event representations are not simply explained only by items within event sharing the same color background alone, as items from different events that shared the same background color (but were not continuous in time) were not represented similarly in CA3 (Rep5: $\chi^2_{(1)} = .33, p = .57$). Together, these results provide strong evidence for distinct event representations in hippocampal area CA3.

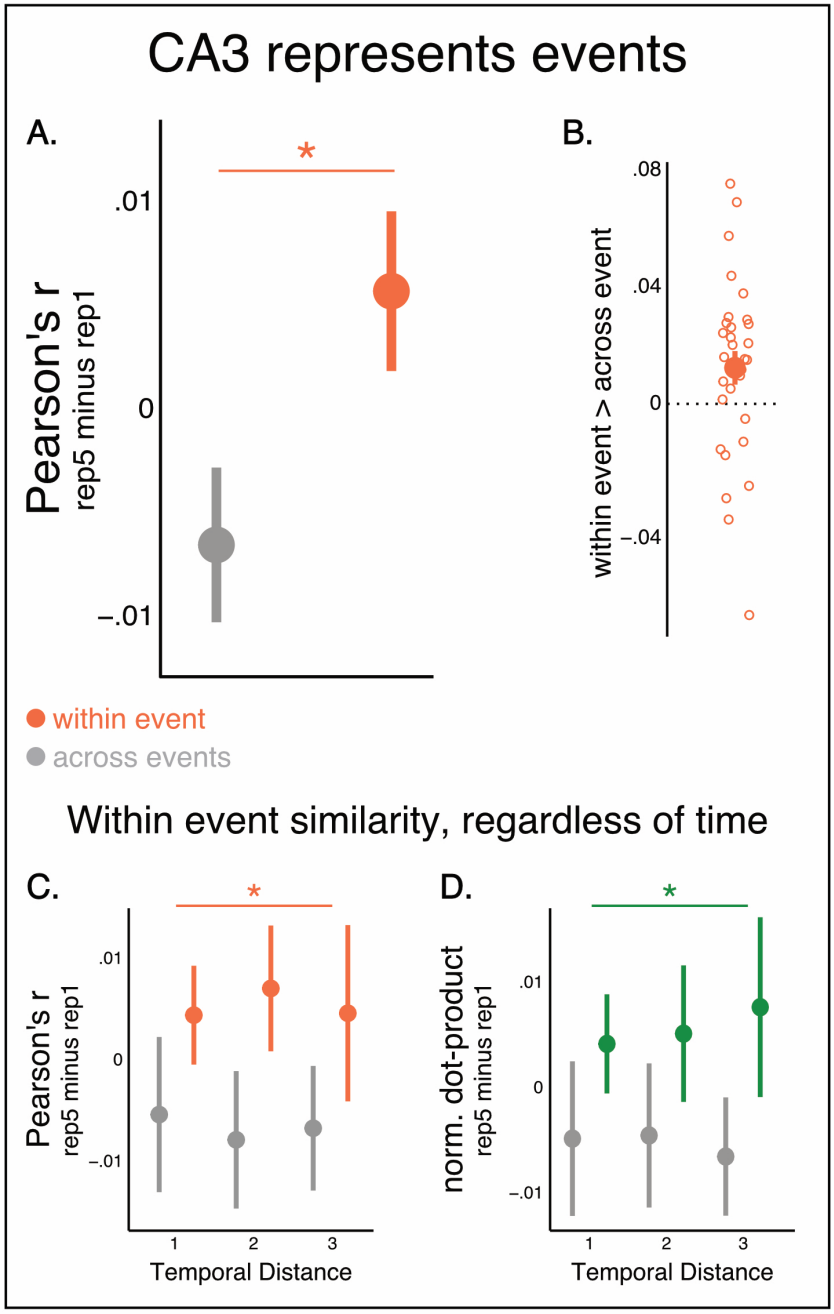

Figure 3. left CA3 activity patterns represent events. A. Similarity values (Pearson's r) within event (orange) and across events (grey) in CA3. Rep5: 5th repetition, Rep1: 1st repetition. B. Individual participants' values of the difference between within event and across events similarity. C. the same data as in A, but presented per each level of temporal distance. As can be seen, similarity did not differ based on temporal distance in CA3. D. Same as C but using normalized dot-product values. N = 30. Data are presented as mean values, error bars reflect +/- SEM. * p = .02, reflecting higher similarity within compared to across events, collapsed across gaps (statistical analysis was conducted by entering similarity values of individual pairs to linear mixed-effects models and conducting model comparisons using Chi-square tests, see main text).

CA3 event representations facilitate transitioning between events

We asked, if event representations in CA3 distinguish nearby events by allocating them to distinct neuronal ensembles, what consequences if any, might have on behavioral segmentation? As mentioned above, RTs at event boundaries items are slower compared to non-boundary items, which has previously been interpreted as a behavioral marker of event segmentation (Heusser et al., 2018; Pettijohn & Radvansky, 2016; Zacks, 2020). One possibility is that the strength of event representations in CA3 may facilitate transitioning between events. To examine this, we created a metric of neural clustering to index distinct representations of adjacent events by averaging similarity within each of two adjacent events and subtracting from it the similarity across these same events (see Methods). Neural clustering was then regressed with the transition cost: the difference between the RT to the boundary item in the second of these events and the immediately preceding pre-boundary item (the subtraction measure per event-pairs allows a closely controlled within-participant correlation, see Methods). As can be seen in Figure 4, we found greater neural clustering in the left CA3 significantly correlated with less cost at the boundary, namely, smaller RT difference between the pre-boundary and boundary items in repetition 5 ($\chi^2_{(1)} = 8.56$, $p = .003$, AIC reduction: 6.56). If neural clustering facilitates transitioning between events, it should be driven by the similarity across events, and RTs at the boundary. Indeed, lower similarity across events (more distinction) significantly correlated with faster RTs at the boundary ($\chi^2_{(1)} = 5.28$, $p = .022$, AIC reduction: 3.28). Similarity within event did not explain RTs at the boundary at the pre-boundary item, nor did similarity across events explain RTs for pre-boundary items ($\chi^2_{(1)}$'s < 1.6, p's > .21). This result suggests that, for well-learned events, distinct event representations in CA3 facilitate transitioning between events.

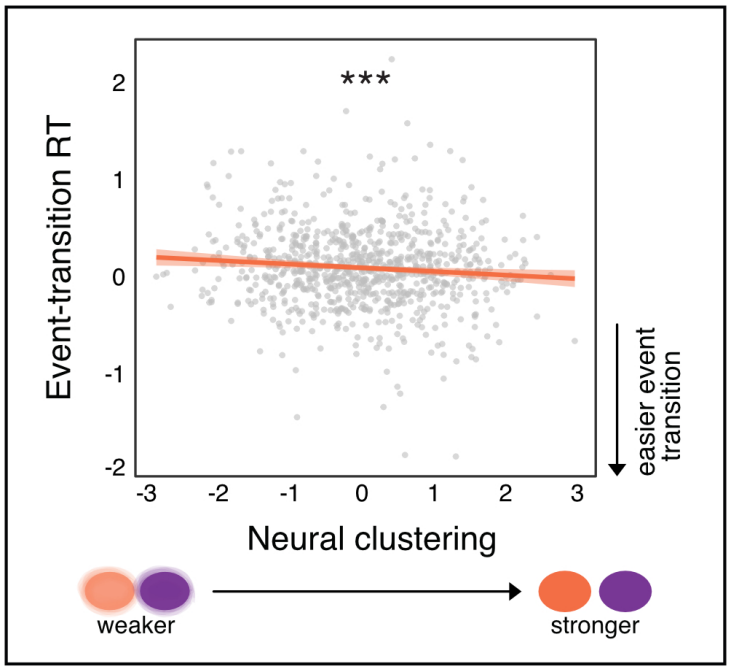

Figure 4. Neural clustering in the left CA3 correlates with easier event-transitions. The difference between CA3 similarity within event and CA3 similarity across events (i.e., Neural clustering) correlated with easier transition between events, as reflected by a smaller difference between RTs for boundary and pre-boundary items. Data are from the 5th repetition, each dot reflects values per participant per event. Similarity values are scaled within participant. *** p = .003, results of model comparisons using Chi-square test for comparing between mixed-level models.

CA3 representations reflect the involvement of different populations of voxels

So far, we see greater CA3 neural pattern similarity within events compared to across events and that the extent of neural event clustering facilitates event transition, as measured in response times. We next assessed the extent to which these results are consistent with adaptive attractor dynamics, in which different events are represented by different populations of CA3 neurons (Kesner & Rolls, 2015; Knierim & Neunuebel, 2016; Treves & Rolls, 1994). In fMRI, the unit of measure is a voxel so we could ask whether different voxels are engaged for distinct events. While the data reported above shows learning related emergence of event representations, the correlation measure used (and that is prevalent in RSA studies), while capturing changes in the population of voxels activated for an item, can also be sensitive to changes in overall activation level in only a subgroup of voxels. That is because when activation levels in a subgroup of voxels changes, the mean activation level across the entire group of voxels changes correspondingly. Consequentially, the distance from the mean of each voxel changes, and with it the value of the correlation (note that this is true for Spearman's correlation as well, not just Pearson's correlation). Thus, we computed

additional measures of representational similarity that are (1) sensitive to the overlap in the population of active voxels versus the level of activation, and (2) sensitive to changes in activation levels, regardless of the population of voxels involved.

To that end, we adopted two known similarity measures, normalized dot product and the norm difference, that have been previously used in rodent work, to fMRI (Madar et al., 2019). The normalized dot product is the cosine of the angle between two activity patterns (higher means more similar), normalized by their norms (the sum of squared activation values across all voxels), which makes it robust to changes in levels of activation, even in some voxels. The norm difference is the difference between the norms of two activity patterns, thus it is only sensitive to differences in level of activation and is blind to the population of voxels contributing to that difference (see Methods). Simulations we conducted show that changing activation levels in some voxels of non-overlapping patterns influence Pearson's correlation and the norm difference, but not the normalized dot product, while changing the overlap between patterns while holding activation levels constant influence both Pearson's correlation and the normalized dot product, but not the norm difference (schematic description in Figure 5, for detailed results and additional simulations, see Supplementary Information and Supplementary Figure 6).

Computing the normalized dot product and norm difference on our fMRI data, we anticipated we would replicate our correlation results in the normalized dot product measure but see no differences between the patterns' norms. Indeed, the normalized dot product replicated our Pearson's correlation results, finding higher similarity within compared to across events in the 5th repetition (main effect of Event, within vs. across event: $\chi^2_{(1)} = 4.56$, $p = .03$, AIC reduction: 2.56), with no difference based on temporal distance (main effect of Temporal Distance: $\chi^2_{(1)} = 0.017$, $p = .89$; Event by Temporal Distance interaction: $\chi^2_{(1)} = 0.17$, $p = .68$; Figure 3). No effect of Event,

Temporal Distance nor an interaction were observed in the norm-difference measure ($\chi^2_{(1)}$'s < .60, p's > .43). Note that the norm difference does not reflect average activation, but the sum of squared activation differences between activity patterns. Thus, it is unlikely that lack of a difference stems from some voxels reducing activations, while others increasing their activation – this should have led to a major difference in norm difference. Together, the results from the normalized dot product and the norm difference measures provide further evidence that similar populations of voxels represent items belonging to the same events, while different events are represented using different populations of voxels, consistent with attractor dynamics.

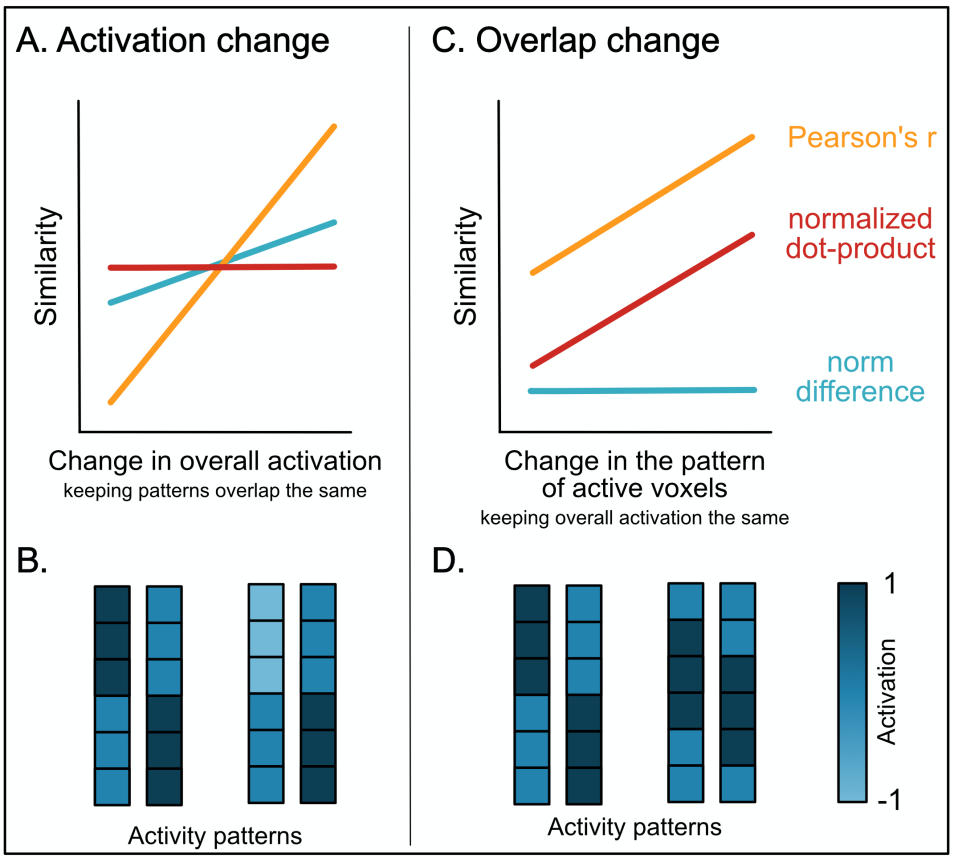

Figure 5. Schematic of the simulations of Pearson r, normalized dot product, and norm difference measures. A. When active voxels do not overlap, changing the level of activation in a subgroup of voxels led to differences in Pearson's r and norm difference, but not in the normalized dot-product. B. Activity patterns showing the change in a subgroup of voxels. C. Altering the voxels' overlap, without changing their level of activation, led to a change in Pearson's r and normalized dot-product, but not in norm difference. D. Activity patterns showing the change in overlap of active voxels across both activity patterns. See more details in the main text in the Supplementary Information.

Temporal pattern separation in the left DG is sensitive to context

We now turn to the left DG. As above, similarity values between activity patterns of objects with temporal distance of 1, 2, 3, both within and across events, were entered to mixed-level models. In the left DG, we found a significant interaction between Event and Temporal Distance ($\chi^2_{(1)}$ = 6.37, p = .01, AIC reduction: 4.37), stemming from lower pattern similarity between objects presented close in time, and only so if they were experienced within the same event (Figure 6, Supplementary Figure 2). Temporal Distance significantly explained variance within events, but not across events (within event: $\chi^2_{(1)}$ = 11.18, p = .0008, AIC reduction: 9.18; across events: $\chi^2_{(1)}$ = .14, p > .71). We refer to this as *temporal pattern separation*, and suggest that in the left DG, temporal pattern separation is specific to objects appearing within the same event, that is, the same context.

We next examined learning related changes in temporal pattern separation. To that end, pattern similarity values from left DG was entered to a mixed-level model testing the interaction of Event, Temporal Distance, and Repetition. This revealed a significant 3-way interaction ($\chi^2_{(1)}$ = 4.68, p = .03, AIC reduction: 2.68), suggesting that the modulation of left DG neural pattern similarity by Temporal Distance and Event changed through learning. To better understand these changes, we followed up on this 3-way interaction by analyzing the 2nd and 5th repetitions separately. In the 2nd repetition, we found no interaction of Event by Temporal Distance, nor a main effect of Temporal Distance, either within or across events (Interaction: $\chi^2_{(1)}$ = .02, p = .88, main effects of Temporal Distance within, across events: $\chi^2_{(1)}$'s < 1.1, p's > .30). However, in the 5th repetition there was a significant interaction of Event by Temporal Distance ($\chi^2_{(1)}$ = 6.27, p = .01, AIC reduction: 4.27). Pattern similarity was lower for objects close vs. far in time within event, but not across events (within event, main effect of Temporal Distance: $\chi^2_{(1)}$ = 10.21, p =

.001, AIC reduction: 8.21; lag of 1 vs. 2: $\chi^2_{(1)} = 5.59$, $p = .02$, AIC reduction: 3.59; lag of 1 vs. 3: $\chi^2_{(1)} = 8.11$, $p = .004$, AIC reduction: 6.11; the same comparisons across events: $\chi^2_{(1)}$'s < .23, p's > .63). These results remained the same accounting for univariate activation (Supplementary Information). We further note that temporal pattern separation between objects that are close in time seemed stable across the different positions in the event (Supplementary Figure 3). To sum up, through learning, items that were close in time and belonged to the same event, and thus potentially shared similar temporal and perceptual information, became more separated in the left DG (Kesner, 2018; S. Leutgeb & Leutgeb, 2007; O'Reilly & McClelland, 1994; Treves & Rolls, 1994; Yassa & Stark, 2011).

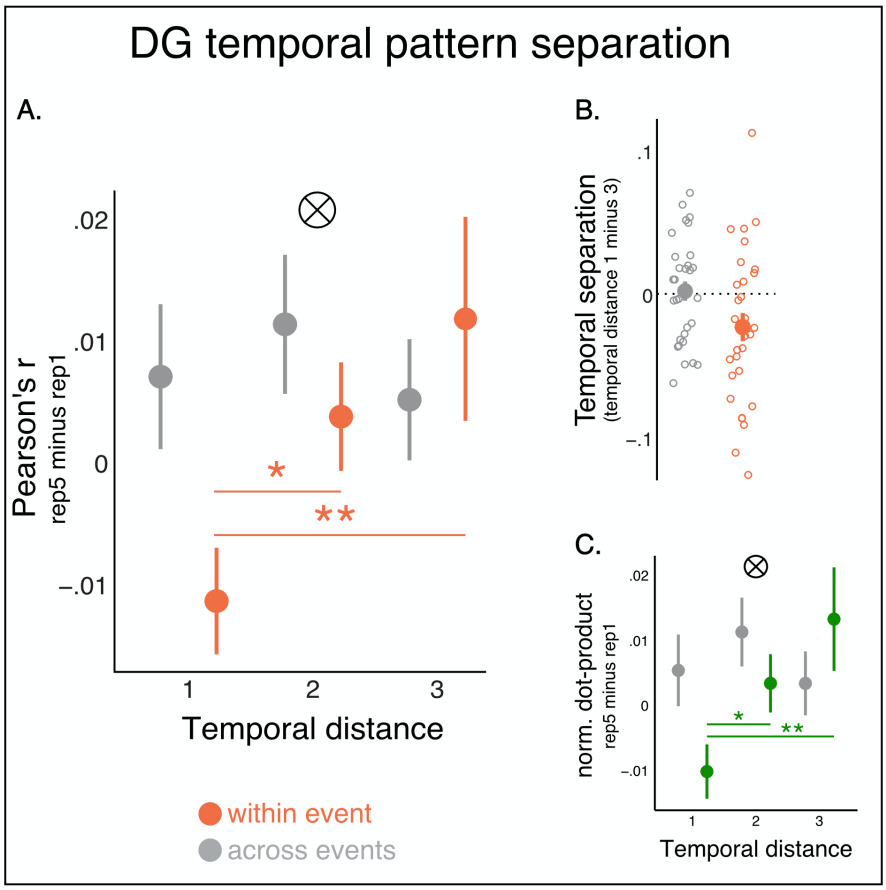

Figure 6. Dentate gyrus (DG) activity patterns reflect temporal pattern separation within events. A. Similarity values (Pearson correlation) in DG within event (orange) and across events (grey). Rep5: 5th repetition, Rep1: 1st repetition. B. Individual participants' temporal pattern separation: the difference in pattern similarity between temporal distance of 1 object versus 3 objects, separately for within vs. across events. C. Same as A, but using the normalized dot-product values. Data are presented as mean values, error bars reflect +/- SEM. ⊗ p <= .01, Interaction of Event (within vs. across) by Temporal Distance, * p = .02, ** p = .004. Statistical analysis was conducted by entering similarity values of individual pairs to linear mixed-effects models and conducting model comparisons using Chi-square tests. N = 30.

A dynamic inhibition model for temporal pattern separation in DG

What mechanism can underly temporal pattern separation in DG? We suggest that inhibitory dynamics may account for lower similarity between temporally adjacent items (Figure 7; Hasselmo & Wyble, 1997; Kesner & Rolls, 2015; Myers & Scharfman, 2011). Specifically, we propose the DG neurons that are activated for one item (e.g., item n) become inhibited for some time such that they are not active when the immediately following item (n+1) appears. This results in other neurons representing the n+1 item, and in low overlap between activity patterns of temporally adjacent items (items n and n+1). Inhibition then gradually decays, so that for the following item (n+2), some of the neurons can overcome this inhibition and are active again, resulting in slightly higher correlation between items n and n+2. By item n+3, inhibition decays enough such that similarity levels are high again and reach the levels of between-event similarity. Between events, this inhibition between DG neurons does not come into play because items can be distinguished based on perceptual features alone, thus DG pattern separation is unnecessary (see Discussion). This can potentially be mediated by inhibitory and excitatory signals reaching DG from its input regions to control pattern separation (Myers & Scharfman, 2011; Scharfman, 2007). Since the specific mechanism is beyond the scope of the current paper (though see below CA3-DG connectivity results), we simply turn off inhibition between events in the following model. We implemented dynamic inhibition within events in a simple computational model, simulated the resulting activity patterns, and computed the similarity between these activity patterns (Methods). We do not aim to offer a comprehensive mechanistic account (but see Discussion). Rather, our primary goal was to illustrate that the ideas detailed here indeed result in the pattern of the data we observed in the left DG. As can be seen in Figure 7, indeed, when we plot the pattern similarity from the model outputs, the results show the same temporal pattern

separation that aligns with our empirical data, providing a proof of concept for our dynamic inhibition model (for full results see Supplementary Figure 4).

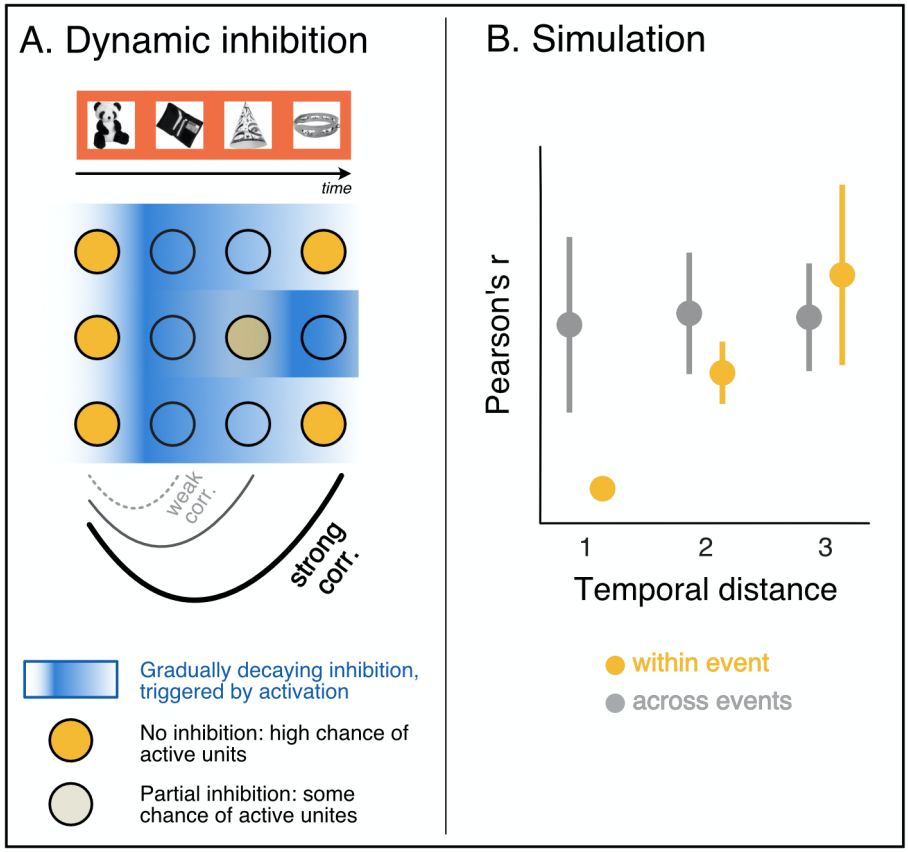

Figure 7. Dynamic Inhibition model for temporal pattern separation in DG. A. Activated units (yellow circles) trigger inhibition that is maximal in the next trial (n+1) but then gradually decays (blue to white background). By trial n+2, partial inhibition leads to some chance for a unit to be activated again (faded yellow). By trial n+3 there is no inhibition, and therefore a unit has a higher chance of being active. The curves reflect the resulting correlation between activity patterns. D. Similarity (Pearson correlation) between simulated activity patterns based on the dynamic inhibition model, resembling our empirical data (details in the Methods).

DG pattern similarity reflect the involvement of different populations of voxels

The dynamic inhibition model suggests that activation of different population of units, and in our case, voxels, might underly temporal pattern separation. Thus, we used the additional similarity measures developed above (normalized dot product and norm difference) to strengthen the empirical evidence that different populations of voxels, rather than changes in level of activation (potentially in a subgroup of voxels), underlies the results observed in DG. As above, if the pattern similarity results reflect changes in the activation of distinct voxels and not in the activation level of the same voxels, we predicted that we would replicate our correlation results in the normalized dot product measure, but not in norm differences. Indeed, mean normalized dot product values in

the left DG showed a similar pattern to the Pearson's correlation: lower normalized dot product for items that are close in time, only within event, but not across events (Figure 6). As in Pearson's correlation, in the 5th Repetition, the interaction between Event and Temporal Distance was significant ($\chi^2_{(1)} = 6.77$, $p = .009$, AIC reduction: 4.77). Temporal Distance significantly explained variance within event, but not across events (within event: $\chi^2_{(1)} = 10.429$, $p = .001$, AIC reduction: 8.43; across events: $\chi^2_{(1)} = .33$, $p > .56$). Critically, we found no difference based on temporal distance or events, or their interaction in the norm difference measure (all p's > .14). Together, the results from the normalized dot product and the norm difference measures provide further evidence that temporally close items within the same event are represented by different populations of voxels in the left DG. These results are consistent with the dynamic inhibition model.

CA3-DG connectivity increases with learning

A prominent theoretical model has proposed that inhibition in DG, and consequentially pattern separation, is achieved via back-projections from CA3 (Myers & Scharfman, 2011). So far, we have found that temporal pattern separation in DG increased with learning (see above). If pattern separation is mediated via CA3 back-projections and was higher in repetition 5 compared to early in learning, we aimed to examine if a concomitant increase in CA3-DG synchronization is evident from the first to the 5th learning repetition. To address that, we used a background connectivity approach which has been previously used to characterize circuit dynamics in hippocampal subfields during different phases of learning (Duncan, Tompary, & Davachi, 2014; Tompary, Duncan, & Davachi, 2015). We found that functional connectivity between CA3 and DG did indeed significantly increase from the first to the 5th repetition (1st rep: $M = .34$, $SD = .24$; 5th rep:

M = .49, SD = .23, $t_{(29)}$ = 3.07, p = .005, Cohen's d = .56; see Supplementary Figure 5 for data from all repetitions).

Discussion

Decades of research have shown that the brain segments continuous experience into discrete events based on context (Clewett & Davachi, 2017; Gernsbacher, 1985; Radvansky & Zacks, 2017; Schank & Abelson, 1977; Zacks, 2020; Zacks et al., 2007). The hippocampus is central to event cognition (Ben-yakov & Henson, 2018; Clewett et al., 2019; Maurer & Nadel, 2021; J. Zheng et al., 2022), potentially through its role in representing contextual and sequential information (Bellmund et al., 2020; Buzsáki & Moser, 2013; Buzsáki & Tingley, 2018; Davachi & DuBrow, 2015; Deuker et al., 2016; Eichenbaum, 2017; O′Keefe & Nadel, 1978; Ranganath & Hsieh, 2016; Rueckemann et al., 2021; Umbach et al., 2020). Critically, the hippocampus does not merely create copies of the external environment. Rather, it creates integrated representations of related life events, potentially allowing generalization and inference, while at the same time facilitating separated neural representations to distinguish memories (Brunec et al., 2020; Duncan & Schlichting, 2018; Liu et al., 2022; Molitor et al., 2021; Sugar & Moser, 2019). Theory and empirical data implicate the CA3 subregion of the hippocampus in integration and the DG subregion in separation (Knierim & Neunuebel, 2016; Marr, 1971; O′Reilly & McClelland, 1994; Treves & Rolls, 1994; Yassa & Stark, 2011). However, how time and context shape integration versus separation in hippocampal subregions to structure event representations, and how these representations change with learning, is unknown.

Here, participants learned repeating events while undergoing high-resolution fMRI. Event structure was evident in participants behavior, reflected in slower RTs for boundary items during

learning, and slower RTs in a temporal memory test when memories bridged across different events. Using high-resolution fMRI and multivoxel pattern similarity analysis, we found that CA3 activity patterns within the same event were more similar compared to across events, irrespective of temporal distance, suggesting that CA3 clustered representations based on events. The strength of neural event clustering in CA3 correlated with faster RTs during event transitions, suggesting that CA3 clustering facilitated transitioning between events. This adaptive CA3 segmentation is consistent with an attractor dynamics account for CA3. In contrast to CA3, DG showed greater separation between objects that were close in time, compared to further in time, and only if objects were experienced in the same event. Thus, DG may perform pattern separation of temporally proximal information during an event, to facilitate distinct representations of subevent elements. A dynamic inhibition model, proposing that activated units are temporarily inhibited and then gradually released form inhibition, accounted for DG temporal pattern separation. In both CA3 and DG, integrated and differentiated event representations strengthened with learning. Finally, newly developed similarity measures provided supporting evidence that different population of voxels contributed to changes in similarity in both regions, consistent with attractor dynamics in CA3 and dynamic inhibition in DG. These findings provide novel empirical evidence for theoretical models of hippocampal computations (Knierim & Neunuebel, 2016; Marr, 1971; O′Reilly & McClelland, 1994; Treves & Rolls, 1994; Yassa & Stark, 2011) and advance our understanding of how the hippocampus hierarchically represents learned sequences in time and context (Bellmund et al., 2018; Buzsáki & Tingley, 2018; Davachi & DuBrow, 2015; de Sousa et al., 2021; Eichenbaum, 2017; Jafarpour et al., 2019; Theves et al., 2021).

CA3 event representations emerged even though the task allowed integration across different contexts. Specifically, in the current study, the order of objects and hence sequential

events was replicated in the five learning lists. This theoretically offered participants the opportunity to predict and, thus, sequentially link across events even with the change in context features. From one perspective, that event segmentation arises from a prediction error process (Franklin et al., 2020; Zacks, 2020; Zacks et al., 2007, 2011), we might have expected to see a reduction in segmentation over learning repetitions. Instead, behavioral markers of segmentation were still evident in the fifth repetition, and CA3 neural clustering was even stronger, suggesting that event segmentation is a process used and applied even when events are highly predictable. Consistent with this, previous studies have found evidence for hippocampal event representations in highly predictable environments (Hindy et al., 2016; Hsieh et al., 2014; Kok & Turk-Browne, 2018; Kyle, Stokes, et al., 2015; Schapiro et al., 2012, 2016). But, they used paradigms in which the target sequence was determined by high predictability compared to low predictability between sequences, thus learning the predictability structure was the only way of segmenting sequences into events (Hsieh et al., 2014; Schapiro et al., 2012, 2016). Other studies trained participants on discrete sequences or environments, requiring no segmentation (Hindy et al., 2016; Kok & Turk-Browne, 2018; Kyle, Stokes, et al., 2015; Liu et al., 2022; L. Zheng et al., 2021). By contrast, in our study, the fixed order made transitions within and across events fully and equally predictable, such that participants could learn and integrate across events. Nevertheless, participants leveraged the predictability in the list structure to adaptively chunk events instead of integrating across event boundaries (Clewett & Davachi, 2017; Shin & DuBrow, 2021).

An interesting question is whether CA3 similarity of activity patterns is stable through events, potentially reflecting stability of temporal context, or whether high similarity stems from reactivation of event components during, e.g., event boundaries (Davachi & DuBrow, 2015; Horner et al., 2015). A prominent context model of CA3 suggests that CA3's auto-associative

network leads to maintenance of an internal context representation. This context representation is then linked to items in that context, promoting similarity in neural representation of components of the same event (Hasselmo & Eichenbaum, 2005), and echoing computational cognitive models implementing temporal context as a slowly drifting representation (Howard & Kahana, 2002; Lohnas et al., 2015; Polyn et al., 2009). Consistent with a contextual stability account, previous studies in rodent and humans found that the similarity of hippocampal representations during learning correlated with temporal memory of these events (DuBrow & Davachi, 2014; Ezzyat & Davachi, 2014; Lositsky et al., 2016; Manns et al., 2007; Umbach et al., 2020; but see Jenkins & Ranganath, 2016, for reviews, see Clewett et al., 2019; Clewett & Davachi, 2017; DuBrow & Davachi, 2017; Long & Kahana, 2019). Alternatively, a reactivation account for CA3 would propose that, upon encountering a part of an event, the auto-associative network in CA3 promotes the reactivation of additional event components (Davachi & DuBrow, 2015; Horner et al., 2015; Knierim & Neunuebel, 2016; Marr, 1971; O′Reilly & McClelland, 1994; Schapiro et al., 2012; Treves & Rolls, 1994). In this account, some subevent components may trigger reactivation more than others. To our knowledge, previous work has not specifically examined CA3, nor has similarity throughout the entire event been examined (Deuker et al., 2016; DuBrow & Davachi, 2014; Ezzyat & Davachi, 2014; Jenkins & Ranganath, 2016; Kalm et al., 2013; Thavabalasingam et al., 2018, 2019), which is crucial to distinguishing between context maintenance versus reactivation of event components. While not the purpose of this study, an exploration of our data revealed that similarity values were numerically higher at event edges (i.e., the boundary item and the last item) compared to the middle of the event (Supplementary Figure 3). This was exploratory, and not statistically significant. However, it provides some evidence for the reactivation account over context maintenance. Putatively higher similarity at the boundary could reflect prediction of

the coming event (Brown et al., 2016; Hindy et al., 2016; Kok & Turk-Browne, 2018; Schapiro et al., 2012), accompanied by reactivation at the end of the event (Ben-yakov & Dudai, 2011; Cohn-Sheehy et al., 2021; Griffiths & Fuentemilla, 2020; Silva et al., 2019; Sols et al., 2017). One speculation is that there is a shift in hippocampal sequence representations through learning (Ben-yakov et al., 2014; Davachi & DuBrow, 2015), whereby contextual stability during initial learning promote similarity of event representations (DuBrow & Davachi, 2014; Hasselmo & Eichenbaum, 2005; Manns et al., 2007), and these similar representations later facilitate reactivation of learned event components through pattern completion (Grande et al., 2019; Horner et al., 2015; Liu et al., 2022).

In contrast to CA3 event-level representations, DG differentiated the representations of items that were close in time and experienced in same event. These results nicely complement prior theories of the hippocampus (Kesner, 2018; Kesner & Rolls, 2015; Treves & Rolls, 1994; Yassa & Stark, 2011) as well as empirical work in humans showing reduced hippocampal pattern similarity between the multivoxel activity patterns of stimuli that are visually highly overlapping (Chanales et al., 2017; Favila et al., 2016; Koolschijn et al., 2019; Schlichting et al., 2015; Wanjia et al., 2021). or close in narrated, but not actual, time (Bellmund et al., 2022; but see Deuker et al., 2016). Additional studies have reported decreased similarity in CA3/DG between objects that share spatiotemporal context (Copara et al., 2014; Dimsdale-Zucker et al., 2018; Kyle, Smuda, et al., 2015; Liu et al., 2022), and specifically in DG (Berron et al., 2016; see also Baker et al., 2016). Our results extend this prior work in two critical ways: first, we show that DG pattern separation can occur in the temporal domain, thus advancing our knowledge of how temporally extended experiences are represented in the brain (Davachi & DuBrow, 2015; Eichenbaum, 2014). Second, our results suggest that temporal pattern separation is sensitive to context: DG does not separate

all temporally similar experiences, but only when these experiences share the same context. Like the CA3 findings suggesting integration of temporally extended events, the DG temporal pattern separation results suggest that the hippocampus does not merely represent sequences as an accurate copy of external experience. Rather, the hippocampus edits events, creating integrated and separated representations that are putatively adaptive for behavior (Ben-yakov & Henson, 2018; Clewett et al., 2019; Ezzyat & Davachi, 2014; Madar et al., 2019; Sugar & Moser, 2019).

Using a simple computational model, we suggest that inhibitory dynamics in DG may underlie temporal pattern separation (Hasselmo & Wyble, 1997; Kesner & Rolls, 2015). Potentially, units (neurons, or voxels) that are activated in one item, are then inhibited in the following item, maximizing separation between items. Then, this inhibition gradually decays, resulting in gradually decaying separation (Figure 7). This suggestion is consistent with a prominent and biologically plausible computational model that specifies how reactivation of competitors leads to their subsequent inhibition (Norman et al., 2006) and to differentiation in their neural representations (Hulbert & Norman, 2014; Kim et al., 2017; Molitor et al., 2021; Ritvo et al., 2019). Another, not mutually exclusive model, proposes that back-projections from CA3 inhibit DG neurons, and facilitate pattern separation (Myers & Scharfman, 2011). Future research could investigate the specific mechanism by which temporal pattern separation may arise in the DG.

Many previous representational similarity studies in humans collapsed across CA3 and DG (Dimsdale-Zucker et al., 2018; Hindy et al., 2016; Kok & Turk-Browne, 2018; Kyle, Stokes, et al., 2015; Liu et al., 2022; Schapiro et al., 2012; Schlichting et al., 2015; Stokes et al., 2015; Wanjia et al., 2021; L. Zheng et al., 2021), hindering the examination of differences in these regions' putative functions, namely CA3 integration through attractor dynamics compared to DG pattern

separation (Kesner & Rolls, 2015; Marr, 1971; Treves & Rolls, 1994; Yassa & Stark, 2011). Here, we leveraged a widely accepted automatic segmentation protocol of hippocampal subfields (Iglesias et al., 2015), in combination with automated alignment of the ROIs from anatomical to functional space (Methods). In our fMRI data, we were able to dissociate CA3 and DG in two different measures: average BOLD activity and pattern similarity. Thus, while we do not wish to argue that we have achieved perfect anatomical segmentation, our segmentation procedure was useful to uncover compelling functional distinctions. Future studies, for example using 7T fMRI, will be important to confirm these findings. However, our novel procedure has clear advantages: it is available to any 3T scanner user, and it is fully automated, which is efficient and reproducible.

In sum, in the present study we examined learning of temporally extended events and found that CA3 integrated items within event, and separated across events, consistent with an attractor dynamics account. DG, in contrast, separated representations for items that were close in time and within the same context, consistent with temporal pattern separation that is sensitive to context. These results show how the hippocampus hierarchically represent events to address a major challenge of our memory system: how to integrate information to build contextually relevant knowledge, while maintaining distinct representations of this same information (Brunec et al., 2020; Duncan & Schlichting, 2018; McKenzie et al., 2014; Tompary & Davachi, 2017). Through learning, such hierarchical event representations can become the building blocks of organized semantic representations, including schemas, categories, and concepts (Collins & Quillian, 1969; Eichenbaum, 2004; Garvert et al., 2017; Ghosh & Gilboa, 2014; Mack et al., 2018; Morton et al., 2017; Murphy, 2004; Nieh et al., 2021; Renoult et al., 2019; Theves et al., 2021; Tulving, 1972). How event representations as observed here are transformed to become schematic knowledge is

an exciting question for future research (Gilboa & Moscovitch, 2021; Moscovitch et al., 2016; Robin & Moscovitch, 2017; Tompary & Davachi, 2017).

Author contributions

O.B. and L.D. conceptualized the experimental design and analytical approach. O.B. collected and analyzed the data. O.B. wrote an initial draft of the paper, O.B. and L.D. revised and edited the paper. L.D. supervised and obtained funding.

Data and code availability

Data will be available upon a reasonable request from the authors. Code will be available upon publication.

Acknowledgements

This research was supported by the National Institute of Mental Health Grant R01MH074692 to L.D. O.B. was further supported by a McCracken fellowship and a Grinker award. We thank Andrew Heusser and J. Quinn Lee for help in initial conceptualization of the behavioral paradigm, and Natalie Plotkin and Adam Benzekri for their help in behavioral piloting of the task. We thank Monika Riegel, Tarek Amer and David Clewett for insightful comments and conversations, and Emily Cowan, Tarek Amer, Camille Gasser, and John Thorp for comments on earlier drafts of the manuscript.

Methods

Participants. Thirty participants were included in this study (18 females, aged 18-35 years, mean age: 23.32). One additional participant was excluded due to exceeding movement (more than 3 mm within a scan, as indicated by MCFLIRT estimated mean displacement; most participants had below 1.5mm movement in all scans, one participant had one scan with 3mm displacement, our examination revealed that MCFLIRT could correct this motion to .6mm motion, which is within voxel. Hence, this participant was included). Two additional participants were excluded due to

poor compliance with the task (lower than 2.5SD of the group average in the temporal memory test, during the first or the second day of testing). The sample size of 30 was determined based on previous fMRI studies using similar approaches (Aly et al., 2018; Dimsdale-Zucker et al., 2018; Schlichting et al., 2015), and a behavioral study using a similar paradigm (Heusser et al., 2018). The participants were members of the New York University community, with normal or corrected-to-normal vision. They were screened to ensure they had no neurological conditions or any contraindications for MRI. The participants provided written informed consent to participate in the study and received a payment at a rate of $30 an hour for the time in the fMRI scanner, and $10 an hour for their time outside the scanner. The study was approved by the New York University Institutional Review Board.

Materials. The stimulus set consisted of 144 gray-scale images of nameable objects on white background, that were selected from a pool previously used in similar studies in our lab (Heusser et al., 2016, 2018). The images were resized to a 350X350 pixels, such that the object occupies as much as possible of that square, and the rest of the square was white. During the list learning phase, objects appeared in the center of a colored squared frame. The size of the color square was 600X600 pixels in total, with the object image covering 350X350 pixels in the center of the square, leaving a frame of 125 pixels around the image of the object. We used 6 colors in the study (brackets refer to the RGB values of the colors): red [255,0,0], green [51,221,0], blue [0,0,255], yellow [255,255,0], orange [255,127,0], and magenta [255,0,255], that were set based on Matlab's 2018 default settings. The background of the screen was set to grey [128,128,128] during all tasks.

Procedure

Overview. The experiment was divided into 2 consecutive days that were identical in their structure. On each day, participants learned three lists of objects. Each list included different objects. During list learning, each list repeated 5 times of identical and immediate repetitions. Before and after the 5 presentations of each list, all objects of that list appeared twice in a random order. The random presentation after the list learning was followed by a temporal memory test for the order of the objects as they appeared during the list learning. On day2, after the temporal memory test of the third list, participants' memory of the object-background color association was tested, for all objects presented on both days. All phases were conducted in the scanner, and were controlled by Matlab (R2018b), using Psychtoolbox3 extensions (Brainard, 1997; Kleiner et al., 2007; Pelli, 1997). On each day, participants received detailed instructions of all phases and practiced them before they entered the scanner and once more in the scanner prior to performing the tasks. Upon completion of all tasks on day2, the participants left the scanner and were shortly debriefed. In the current study we focused on fMRI data from the list learning phase, and behavioral data from the list learning and the temporal memory test. Below, we provide details on each of these tasks.

List learning. Participants learned 6 lists, 3 on each day of the experiment. In each list, participants intentionally encoded 24 gray-scale objects that appeared sequentially, embedded in a colored frame. Objects were unique to each list. On each trial, participants had to visualize the object in the color of the frame and indicate by a button press whether the object-color combination is pleasing or unpleasing to them. Participants indicated by their index or middle finger of their left hand (counterbalanced across participants), using an MRI-compatible response box. The

participants were informed that the decision is subjective and there are no right or wrong answers, and that making this task will help them to remember the color in a later memory task. Each object appeared on the screen for 2 s and was followed by a 3.5 s inter stimulus interval (ISI), and a .5 s fixation cross before the onset of the next trial. The white background and the colored frame remained on the screen continuously (i.e., during the trial and the 3.5 + .5 s ISI and fixation). Participants were asked to make their judgement when the object is still on the screen, although responses were collected also for 1 s after the object was removed from the screen, to allow late responses. The color of the frame was identical for four consecutive objects, before switching to another color for the next 4 objects. The color of the frame switched to the other color simultaneously with the presentation of the first object in an evet. This made every four objects an event with shared context, as manipulated by the frame color (Heusser et al., 2016, 2018). We refer to the first object in an event as the boundary object, appearing in event position 1, followed by non-boundary objects in event positions 2, 3 and 4. There were six events in each list, thus in total participants learned 36 events, in 6 lists. Within each list, the frame alternated between two colors (i.e., events 1, 3, and 5 were of one color, and events 2, 4, and 6 were of the other color in the colors-pair). We used pairs of highly contrasting colors to elicit clear events: red-green, yellow-blue and orange-magenta. Each of these three color-pairs appeared in one list on each day. The allocation of each color to odd-numbered events vs. even-numbered events was randomized for each participant, with the restriction that if a color appeared in odd-numbered events on the first day of the experiment, it would appear in the even-numbered events when the same color-pairs appears in the second day of the experiment, to avoid having identical order of colors across lists (objects were always different across lists). The allocation of each colors-pair to the first, second or third list on each day was also randomized per participant, with the restriction that the first list

on day2 cannot include the same colors-pair as the first list on day1, to prevent participants who might have remembered the color-pairs from the first day to believe that they are going to see exactly the same experiment again on day2. To encourage associative binding of the objects, we instructed the participants to make stories linking the objects together and informed them that this would help them to correctly remember the order of the objects the following temporal memory test (DuBrow & Davachi, 2013). The participants were also provided with an example. Critically, we did not inform or guide them regarding the different events in making the stories. Each list was presented 5 times, immediate and identical repetition. That is, the same 24 objects (6 events) repeated in exactly the same order, with the same color frame. Each repetition was scanned in a separated scan, which began with a 2 s fixation cross (no background and color frame), and ended with a 12 s fixation cross, appearing immediately after the removal of the last object off the screen, to allow estimation of the BOLD response of the last trial.

Temporal memory test. After the 5 repetitions of each list, participants were tested on their memory for the order of the objects. On each trail, participants were first presented with an image of an object from the list, cueing them to recall the following object in the list and hold it in memory. All objects appeared without the colored frame in the memory test. The cue appeared in the center of the screen for 3 s and was followed by a 5 s white fixation cross appearing in the center of the screen. A white fixation cross was used during the delay to orient participants that they still need to hold the following object in memory. Other fixation crosses during this task were black. Then, two objects appeared on the screen next to each other, a target object and a distractor. Participants had to indicate which object immediately followed the cue object during the list learning and rate their confidence. The four response options: “left sure”, “left unsure”, “right unsure”, “right sure”

appeared below the corresponding object on the left/right, and participants indicated their response by pressing one of the corresponding 4 buttons. The participants were asked to respond as quickly as possible without sacrificing accuracy. They were further encouraged to recall the target object during the appearance of the cue and maintain it in their memory, because they might not have sufficient time to recall once the two probes appear on the screen. The appearance of the target on the left or right side was randomized per participant and per list. The distractor was always the object that immediately followed the target object. We used this fine-grained test in which participants had to arbitrate between two very near objects to make sure that our lists were well learned.

We had three types of trials: within event boundary trial, in which the cue was the boundary object, and the target was the object in position 2 (6 trials per list, total of 36 trials in the experiment). This is a within event trial because both the cue and the target appeared in the same event, thus, it tests temporal memory for occurrence within a single event. As within event non-boundary trials, we had trials in which participants were cued with the object in position 2, and the target was the object that appeared in position 3 (6 trials per list, total of 36). We also had across events trials, in which participants were cued with the last object in an event (position 4), and the target item was the first object of the next event (5 trials per list, total of 30). Critically, all objects appeared with and identical temporal distance (i.e., the target immediately followed the cue) during list learning, and the objects were presented during retrieval with no color frame. Thus, the within event and across events trials were identical, only that in across events trials, participants had to retrieve the target from the next event. The order of the trials was pseudo-randomized per participant and per list, such that no object repeats (as a cue, target, or distractor) with a gap of less than one trial. We also verified that the same event will not be tested in any two consecutive trials

(for across events trials, that meant that objects from the event that the cued belonged to, and objects from the event that the target belonged to, did not appear in the previous or next trial). The two probe objects appeared on the screen for 3 s, and were followed by 1 s fixation cross, during which responses were still collected. This was followed by an ITI of additional 3/5/7 s (average 5.25 s), during which participants performed a secondary task: an arrow appeared in the middle of the screen randomly altering between left and right every second. Participants had to indicate the direction of the arrow by a button press. This task was selected to reduce baseline activation levels in the hippocampus between trials, to improve signal estimation (Duncan et al., 2012; Stark & Squire, 2001; note that in the current study, we only report behavioral data from the temporal memory test, this optimization was done for future studies). After the arrows, there was a 1 s fixation, which, 400ms before the onset of the next trial, disappeared for 100ms, and appeared again for another 300ms. This blinking fixation was meant to prepare participants for the next trial, which began with the presentation of the cue. This task as well included a 2 s fixation cross prior to the beginning of the first trial, and a 13 s fixation cross after the 2 probes of the last trial appeared, to allow estimation of the BOLD response of the last trial.

fMRI parameters and preprocessing

Participants were scanned in a 3T Siemens Magnetom Prisma scanner using a 64-channel head coil. The experiment included an MPRAGE T1-weighted anatomical scan (.9X.9X.9mm resolution) and a T2-weighted scan (.9X.9X.9mm resolution) collected on the beginning of day1, prior to any task. Two pairs of fieldmap scans were acquired on each day (in each pair, one scan was acquired in the AP phase encoding direction, the other in the PA phase encoding direction). The first pair was acquired prior to the first list, the second prior to the third list. Each repetition

of each list was conducted in a single whole-brain T2*-weighted multiband EPI scan (77 volumes, TR=2000 ms, 204-mm X 204mm FOV, 136 X 136 matrix, TE=28.6, flip angle=75, phase encoding direction: anterior-posterior, GRAPPA factor 2, multiband acceleration factor of 2). In each volume, 58 slices were acquired tilted minus 20 degrees of the AC-PC, 1.5*1.5*2-mm (width*length*thickness) voxel size, no gap, in an interleaved order. At the end of day2, participants were also given the option of running an additional MPRAGE and T2 scan. These images were collected to ensure having anatomical images in case that the MPRAGE and T2 images collected on day1 were corrupted, but unless mentioned, the day1 images were used for the analysis.

The imaging data were preprocessed using fsl version 5.0.11 (http://www.fmrib.ox.ac.uk/fsl). Images were first corrected for B0 distortion using the acquired fieldmap scans and the topup function. For most optimal correction, we corrected all the scans of each list based on the most nearing fieldmap scans. Thus, the first list on each day was corrected to the first pair of fieldmap scans, while the second and third lists on each day were corrected using the second pair of the fieldmap scans. For three participants, we slightly modified the fieldmap scans we used to adapt for movement detected by the experimenter between runs, but importantly, all scans were corrected for distortion. Following distortion correction, volumes that included motion outliers were detected using fsl_motion_outliers command (framewise displacement, threshold = .9). Preprocessing was conducted using fsl's FEAT (version 6.00). Images were highpass filtered (.1 Hz) and motion corrected within run to the middle volume using MCFLIRT. No smoothing was performed, to protect the boundaries of the hippocampal subfields, and since smoothing is unnecessary for representation similarity analysis (RSA; Kriegeskorte et al., 2006, 2008). All analyses were conducted in each participant's native functional space, and within each

participant's anatomically segmented ROIs. Note that also for the univariate analysis detailed below smoothing was redundant, since we examined average BOLD signal across all voxels in an ROI.

For the analysis of the functional data, we aligned the functional images (for RSA) and the resulting t-stats of the GLMs (for univariate analyses) in each scan to the same functional space within participant, by registering them to a template EPI image. To create this template, for each participant, we averaged together the fieldmap-corrected EPI reference images of the first scan in each day using fsl's AnatomicalAverage command which registers and averages both images (the reference images are single volume images created by the scanner prior to the beginning of the scan, with identical parameters to the functional scan). This averaging across images of both days was done to avoid biasing the registration of images towards one day of the experiment. The MPRAGE image of each participant was registered to the participant's template EPI image using fsl's BBR registration. The transformation matrix created was then used to register the anatomical ROIs to each participant's template EPI image, which is the participant's native functional space.

Regions of Interest

The hippocampal subregions, namely CA3, DG and CA1 (in each hemisphere), as well as CSF and white-matter ROIs to be used as nuisance regressors, were automatically segmented for each participant by Freesurfer 6.0 (Iglesias et al., 2015), using both MPRAGE T1-weigted and the T2-wieghted images. We acknowledge that CA3 and DG are difficult to distinguish (Wisse et al., 2017), and that functional fMRI studies using 3T scanners have so far collapsed across these ROIs (e.g., (Dimsdale-Zucker et al., 2018; Kyle, Stokes, et al., 2015; Tompary et al., 2016), preventing investigation of their different function. We leveraged freesurfer's automatic segmentation and

took a novel and automated approach to register the hippocampal subfields to each participant functional space, with the goal of retaining voxels from small hippocampal subfields to allow representational similarity analysis (RSA, see below).

The anatomically segmented ROIs are masks with 0 or 1 values (1 marks a voxel included in that ROI). When registering these ROIs to the functional space, the alignment and resampling procedure might mix voxels together, such that voxels can have values that are between 0-1. These values reflect the how much of a registered voxel originated in voxels of a value of 1, meaning, voxels that were a part of the anatomical ROI (note that registering the EPI image to the anatomical space creates the same mixture, only without knowing whether or how voxels are mixed, because the original values are not given in 0 or 1. Critically, this further manipulate the functional data. Thus, we registered the anatomical ROIs to the functional space). Per each participant and each hippocampal subfield produced by Freesurfer's anatomical segmentation, we first registered the anatomical ROI mask to the participant's native functional space and thersholded the masks to values of .25. These registered images were than masked by a hippocampus ROI, to ensure that only hippocampus voxels were included in our subfield ROIs. The hippocampus ROI was created by combining all hippocampal subfields detected by Freesurfer, excluding the hippocampal fissure, the fimbria, and the hippocampal-amygdala transition area (HATA). Finally, for each voxel, we assigned the subfield that had the largest value, meaning that this voxel originated mostly in that subfield. Our reasoning was that this approach allows us to functionally dissociate hippocampal subfields (even if not fully distinguish between them), while having the obvious benefits of automatic segmentation and registration procedure, namely, being reproduceable and efficient. Indeed, in both the univariate and the RSA results (see Results) we were able to dissociate CA3 from DG, demonstrating that our methodology was successful in revealing functional

dissociation between these subregions.

The white-matter ROI was aligned to each functional scan, and the mean time-series was extracted from each preprocessed scan using the fslmeants command. To create a confined CSF ROI (Bartoň et al., 2019), we identified, for each participant, a voxel in each hemisphere at the center of the central part of the lateral ventricle and blew a 3mm sphere around that voxel (this was done directly on the template EPI image to make sure we detect the desired voxel in the final functional space, and since the ventricles are clearly visible on EPI). We than masked that ROI with the CSF ROI created by Freesurfer, to further ensure that only CSF voxels were included. The resulting ROI was registered to each functional scan, and the mean time-series was extracted from each preprocessed scan using the fslmeants command.

Quantification and statistical analysis.

Throughout the analyses, of both the behavioral and the neural data, when we used mixed-level models, they were implemented using lme4 package in R (Bates et al., 2015; R core team, 2018). We then used Chi-square test for comparing the models with vs. without the effect of interest to assess significance, and AIC was used for model selection. As all our analyses are within-participant, all models included a random intercept per participant. The models further included a fixed effect of list (as factor) to capture variance related to the different lists.

Behavioral data: list learning. We analyzed reaction time (RT) in making the pleasant/unpleasant task. No responses, too quick responses (below 100 ms), and RTs that were 3 SD above or below the average per participant, list and repetition were excluded from the analysis. On average, 3.19% of the responses were excluded per participant. We also excluded the first response in each list,

which was expectedly much higher compared to the rest of the list. Single-trial RTs were entered as the predicted variable to general linear mixed models (gLMM, as implemented by the glmer function) with inverse Gaussian distribution as the linking distribution function (Lo & Andrews, 2015). We examined the effects of Boundary (boundary/non-boundary objects), Repetition (1-5 as a continuous variable), and their interaction.

Behavioral data: temporal memory test. We analyzed accuracy rates, high-confidence hit rates, and RT. Accuracy and high-confidence hits rates were averaged per participant and entered into a repeated-measures one-way ANOVA with Event Position (Pos1-2, Pos2-3, Pos4-1; Pos1-2, e.g., indicating that participants were cued with an object learned at event position 1, while the following object in event position 2 was the target object; Pos1-2 and Pos2-3 thus tested memory within events, while Pos4-1 trials tested memory across different events, see above). The ANOVA was implemented using the aov function in R stats package, including a within-participant error term i.e., participant/Event Position. To examine RTs, single-trial RTs of high-confidence hits were entered as the predicted variable to general linear mixed models (gLMM, as implemented by the glmer function) with inverse Gaussian distribution as the linking distribution function (Lo & Andrews, 2015). We used only high-confident hits to avoid mixing together different responses, and since high-confidence responses were the vast majority of participants' accurate responses (see Results). The effect of Event Position was tested using all positions in one model, as well as planned comparisons examining the different pairwise comparisons between positions.

Univariate activation. Preprocessed data in each repetition in each list were entered to a voxel based GLM as implemented by fsl's FEAT (version 6.0). We had a regressor per each event

position (4 regressors), which included all the trails in the relevant event position, modeled with 2 s boxcars locked to the onset of each trial that was convolved with FEAT's Double-Gamma HRF function. As nuisance regressors we included the 6 motion regressors as outputted from MCFILRT (3 for translation, 3 for rotation, in each of the x,y,z directions of movement), the average time-series for white-matter and the average time-series of CSF, as well as a regressor for each time-point that was detected as outlier motion by fsl_motion_outliers (this regressor has 1 for the outlier time-point and 0 for all other time-points). To average across different lists within each participant, we registered first level outputs to each participant's native functional space (as detailed above) and ran a second level (participant level) GLM that averages across lists, and thus results in a t-statistic reflecting activation per voxel per event position in each repetition.

For group level analysis, the t-statistics were averaged per participant and per ROI and hemisphere. We quantified each hemisphere separately since previous investigations reported lateralized hippocampal effects (Bein et al., 2020; Dimsdale-Zucker et al., 2018; Kim et al., 2017; Schlichting et al., 2015). Mean activation levels were entered to a repeated measures ANOVA with the factors of Event Position (1-4), Repetition (Rep1/Rep5), ROI (CA3/DG) and Hemisphere (right/left), implemented by aov function in R, including a within-participant error term (participant/Event Position*Repetition*ROI*Hemisphere; note that the aov function wraps around the lm function in R). Follow up repeated measures ANOVAs were conducted within ROI, with the factors of Position, and Repetition, and the relevant within participant error term. Partial eta square was estimated as effect size were relevant (sjstats package, Lüdecke, 2020).

Item-item representational similarity analysis in time and context

To remove nuisance artifacts, preprocessed data was entered to a voxel-based GLM (implemented by fsl's FEAT) with the nuisance regressors as described above: 6 motion regressors as outputted from MCFILRT (3 for translation, 3 for rotation, in each of the x,y,z directions of movement), the average time-series for white-matter and the average time-series of CSF, as well as a regressor for each time-point that was detected as outlier motion by fsl_motion_outliers (default setting; this produces a regressor that has 1 for the outlier time point and 0 for all other time-points per each outlier time point). The residuals of this model were then registered to the template EPI, and the time-course of each voxel within each ROI (CA3, DG), was extracted and z-scored (Kuhl et al., 2012; Kuhl & Chun, 2014). The third TR after the onset of each trial (starting at 4 s after the onset of the trial, capturing the peak of the HRF according to fsl's HRF function, which is ~4 s after the onset; Kim et al., 2017), was extracted from all voxels within an ROI to make the activity pattern corresponding to each trial. Note that this TR is prior to the appearance of the next trial, ensuring that patterns are not contaminated by activity related to the next trial. To clean the data for RSA (Dimsdale-Zucker & Ranganath, 2018), and particularly because correlations are susceptible to outliers, within each participant and each ROI, voxels that demonstrated activation levels exceeding +/-3SD of the mean (across all voxels in an ROI in all lists and repetitions) in a specific trial were removed from all analyses involving this trial.

Within ROI and participant, we then calculated the Pearson's correlation between activity patterns corresponding to each trial and the activity pattern corresponding to all other trials within a list and a repetition, and Fisher-transformed these correlation values. In the current study, we specifically targeted the changes in similarity due to learning, or repetition. Thus, for each correlation value, we subtracted the value of the first presentation. This allowed us to control for

correlations between activity patterns that result from characteristics of the BOLD signal and processing steps (Mumford et al., 2014; Schapiro et al., 2012; Schlichting et al., 2015), which is specifically important when comparing patterns across different temporal gaps, and when the order of the trials cannot be randomized, as in our design (Mumford et al., 2014). Since the lists were identical in all repetitions, subtracting correlation value of the first presentation from the correlation values obtained in the following repetitions alleviates the concern that our results may reflect spurious correlations. Outlier correlation values (+/-3 SD of the mean within each participant) were excluded from the analysis, and the similarity values were entered to group analysis.

The group analysis was conducted by submitting the pairwise similarity values to linear mixed-level models. We took similarity values for temporal distances of 1/2/3 items, i.e., similarity between an object and the immediately following object (lag of 1), as well as the next 2 objects to follow (lag of 2 and 3) in all repetitions. That is because larger distances did not occur within event, only across events. In all models, we included a fixed effect of list and a random intercept per participant.

We first examined whether event representations differed between CA3 and DG. Hemispheres were treated separately due to previous research that reported lateralized representational similarity effects in hippocampal subfields (Bein et al., 2020; Dimsdale-Zucker et al., 2018; Kim et al., 2017; Kyle, Stokes, et al., 2015; Schlichting et al., 2015; Stokes et al., 2015). Thus, the similarity values per pairs of objects were entered to a mixed-effects linear model that examined the interaction between Event (within event/across events), ROI (CA3/DG), and Hemisphere (right/left). Since we observed a significant effect of hemisphere (see Results), we continued to test for the interaction of Event by ROI in each hemisphere separately. Since an

interaction was found in the left hemisphere (see Results), within each of the left CA3 and DG ROIs, we tested the effects of Event, Temporal Distance, and Repetition, and the interaction between these factors. To examine how similarity values may change from early to later in learning, we tested the effect of Event, Temporal Distance, and their interaction in the 2nd or the 5th repetition. Since the observed similarity effects in both CA3 and DG were most pronounced in the 5th repetition, further analyses were limited to the 5th repetition. Further, in all models that did not include temporal distance as an effect of interest, we controlled for temporal distance by including this factor as an explaining variable in the model. Likewise, when testing for the effect of temporal distance, the effect of Event was included in the model to control for within vs. across events differences.

We examined whether left CA3 event representations correlated with behavioral segmentation as participants were learning the lists. To that end, we took the difference between within event and across events similarity in the left CA3 per participant per each two consecutive events, as well as the difference between boundary (Pos1 of the second of the two events) vs. pre-boundary RTs (the preceding Pos4, belonging to the first of the two events). These similarity differences were then entered as an explaining variable to a model, while the RT differences were the predicted variable. These difference scores control for baseline differences and examine whether similarity differences correlated with the relative increase in RTs for the boundary item. The similarity values were scaled within-participant, and as before, a fixed effect of list and a random effect per participant were added. We then followed up on this analysis by examining separately each of the values comprising these difference scores, namely, we examined whether similarity across events, or similarity within event, correlate with RTs of the boundary item (Pos1).

Likewise, we examined whether similarity across events, or similarity within event, correlate with pre-boundary RTs (Pos4 of the first of each two events).

Control for a color background effect in similarity.

As mentioned above, we designed our study in a way that allows us to examine a color effect irrespective of belonging to the same sequential event, because we alternated between two background colors in each list. To examine color effects, we compared a model with a regressor noting "1" for each similarity value between items presented with the same background color and "0" for each pair of items presented with different color, to a model without this regressor. We excluded items within the same event or across adjacent events because these might show higher or lower similarity because they belong to the same or to adjacent sequential event, which, in turn, could artificially contribute to a color effect, given that all items in the same event share the same color, and all items from adjacent events are of different background colors. Temporal distance and list were accounted for in the model as was done above.

Background connectivity analysis

We estimated learning-related changes in background (low frequency) connectivity between CA3 and DG. This approach was previously used to study changes in connectivity between hippocampal subfields at different phases of learning (Duncan et al., 2014; Tambini & Davachi, 2013; Tompary et al., 2015). To remove from the BOLD signal activity directly related to items presented in the task as well as other nuisance factors, we used the residuals of the GLM that modeled univariate activation in each list and repetition of the task (see above), and which included a regressor per each event position, and nuisance regressors of csf and white-matter activity, along

with 6 movement regressors (Duncan et al., 2014). These residuals, reflecting fluctuation in the BOLD signal that are not tied to items in the task, were bandpass filtered into the .01-.035 Hz range using AFNI's 3dBandpass function (Duncan et al., 2014; Newton et al., 2011). This upper threshold is within the range of correlations between grey matter areas in fMRI (Cordes et al., 2001) and further ensures that low-frequency fluctuations do not reflect the event structure of the task, as events changed every 24 s, or .04Hz. To capture changes in connectivity due to learning, the average time course per each list in the first and last presentations (1st Rep, 5th Rep), was extracted per each ROI and participant, and a Pearson's correlation was computed between the time course of CA3 and DG. The resulting correlation coefficients were Fisher-transformed and averaged across lists per each repetition. Thus, they reflect the connectivity between CA3 and DG across each repetition. We used a paired-sample t-test to compare the first presentation (1st rep) and the firth (5th rep). Thus, we directly tested the difference in connectivity between repetitions, which account for baseline connectivity levels between CA3 and DG.

Dynamic inhibition model simulations

Our model generates a random activity pattern for item n, then for the next item (n+1), units active during item n are fully inhibited, thus the patterns are completely non-overlapping. For item n+2, there is full inhibition of units active in item n+1, but only partial inhibition of the units active on item n, meaning we allowed some overlap between activated units in item n and n+2. No inhibition is set on the units of item n during item n+3, or between events. We simulated activity patterns of 2 continuous events, allowing us to examine within and across similarity values. Patterns were set as vectors of 0 (inactive units) or 1 (active units). The portion of active units for each simulated activity pattern was set to .1, or .2 reflecting low levels of activation in DG (Chawla et al., 2005;

Jung & McNaughton, 1993). The simulation starts by allocating a random activity pattern to the item at position 1 in the event. Then, for item 2, we assume full inhibition on the units active for item 1, such that a pattern is generated by randomly selecting a portion of the remaining units (always maintaining overall levels of activation set to .1 or .2). For item 3, the units activated in item 2 are now fully inhibited, whereas the units activated during item 1 are only partially inhibited. To implement partial inhibition, we allowed a percentage of activated units to overlap between item 1 and 3. If a unit was activated, the level of activation was set to 1. The same process repeats for item 4 (only with units active during item 2 partially inhibited, and units active during item 3 fully inhibited). Then, item 1 of the next event is presented to the model and the process starts again, with allocating a random activity pattern to item 1. This effectively turned off inhibition between events. Next, we computed the correlation between these simulated patterns, to compute within and across event similarity values. Overall, we simulated different levels of partial inhibition (.2, .5, .8; as well as levels of 0 or 1 inhibition as a sanity check: zero inhibition should make similarity between item n and n+2 equal to the similarity between item n and n+3, where inhibition is set to 0. Inhibition value of 1 should result in similarity equal to that between item n and n+1, where the inhibition is set to 1; indeed, these patterns were observed, see Supplementary Information and Supplementary Figure 6).

References

Aly, M., Chen, J., Turk-browne, N. B., & Hasson, U. (2018). Learning Naturalistic Temporal Structure in the Posterior Medial Network. *Journal of Cognitive Neuroscience*, *30*(9), 1345–1365.

Aly, M., & Turk-Browne, N. B. (2016a). Attention Stabilizes Representations in the Human Hippocampus. *Cerebral Cortex*, *26*, 783–796. https://doi.org/10.1093/cercor/bhv041

Aly, M., & Turk-Browne, N. B. (2016b). Attention promotes episodic encoding by stabilizing hippocampal representations. *Proceedings of the National Academy of Sciences*, *113*(4), E420–E429. https://doi.org/10.1073/pnas.1518931113

Azab, M., Stark, S. M., & Stark, C. E. L. (2014). Contributions of human hippocampal subfields to spatial and temporal pattern separation. *Hippocampus*, *24*(3), 293–302. https://doi.org/10.1002/hipo.22223

Baker, S., Vieweg, P., Gao, F., Gilboa, A., Wolbers, T., Black, S. E., & Rosenbaum, R. S. (2016). The Human Dentate Gyrus Plays a Necessary Role in Discriminating New Memories. *Current Biology*, *26*(19), 2629–2634. https://doi.org/10.1016/j.cub.2016.07.081

Bakker, A., Kirwan, C. B., Miller, M., & Stark, C. E. L. (2008). Pattern separation in the human hippocampal CA3 and dentate gyrus. *Science*, *319*(5870), 1640–1642. https://doi.org/10.1126/science.1152882

Bartoň, M., Mareček, R., Krajčovičová, L., Slavíček, T., Kašpárek, T., Zemánková, P., Říha, P., & Mikl, M. (2019). Evaluation of different cerebrospinal fluid and white matter fMRI filtering strategies—Quantifying noise removal and neural signal preservation. *Human Brain Mapping*, *40*(4), 1114–1138. https://doi.org/10.1002/hbm.24433

Bates, D., Mächler, M., Bolker, B., & Walker, S. (2015). Fitting Linear Mixed-Effects Models using lme4. *Journal of Statistical Software*, *67*(1). https://doi.org/10.18637/jss.v067.i01

Bein, O., Duncan, K., & Davachi, L. (2020). Mnemonic prediction errors bias hippocampal states. *Nature Communications*, *11*(3451). https://doi.org/10.1038/s41467-020-17287-1

Bellmund, J. L. S., Deuker, L., Montijn, N. D., & Doeller, C. F. (2022). Mnemonic construction and representation of temporal structure in the hippocampal formation. *Nature Communications*, *13*(1), 3395. https://doi.org/10.1038/s41467-022-30984-3

Bellmund, J. L. S., Gärdenfors, P., Moser, E. I., & Doeller, C. F. (2018). Navigating cognition: Spatial codes for human thinking. *Science*, *362*(6415). https://doi.org/10.1126/science.aat6766

Bellmund, J. L. S., Polti, I., & Doeller, C. F. (2020). Sequence Memory in the Hippocampal-Entorhinal Region. *J. Cogn. Neurosci.*, *32*(11), 2056–2070. https://doi.org/10.1162/jocn_a_01592

Ben-yakov, A., & Dudai, Y. (2011). Constructing Realistic Engrams: Poststimulus Activity of Hippocampus and Dorsal Striatum Predicts Subsequent Episodic Memory. *Journal of Neuroscience*, *31*(24), 9032–9042. https://doi.org/10.1523/JNEUROSCI.0702-11.2011

Ben-yakov, A., & Henson, R. N. (2018). *The Hippocampal Film Editor: Sensitivity and Specificity to Event Boundaries in Continuous Experience*. *38*(47), 10057–10068.

Ben-yakov, A., Rubinson, M., & Dudai, Y. (2014). Shifting Gears in Hippocampus: Temporal Dissociation between Familiarity and Novelty Signatures in a Single Event. *Journal of Neuroscience*, *34*(39), 12973–12981. https://doi.org/10.1523/JNEUROSCI.1892-14.2014

Berron, D., Schutze, H., Maass, A., Cardenas-Blanco, A., Kuijf, H. J., Kumaran, D., & Duezel, E. (2016). Strong Evidence for Pattern Separation in Human Dentate Gyrus. *Journal of Neuroscience*, *36*(29), 7569–7579. https://doi.org/10.1523/JNEUROSCI.0518-16.2016

Bird, C. M. (2020). How do we remember events? *Current Opinion in Behavioral Sciences*, *32*, 120–125. https://doi.org/10.1016/j.cobeha.2020.01.020

Brainard, D. H. (1997). The Psychophysics Toolbox. *Spatial Vision*, *10*(4), 433–436.

Brown, T. I., Carr, V. A., LaRocque, K. F., Favila, S. E., Gordon, A. M., Bowles, B., Bailenson, J. N., & Wagner, A. D. (2016). Prospective representation of navigational goals in the human hippocampus. *Science*, *352*(6291), 1323–1326. https://doi.org/10.1126/science.aaf0784

Brown, T. I., Hasselmo, M. E., & Stern, C. E. (2014). A high-resolution study of hippocampal and medial temporal lobe correlates of spatial context and prospective overlapping route memory. *Hippocampus*, *24*(7), 819–839. https://doi.org/10.1002/hipo.22273

Brown, T. I., & Stern, C. E. (2013). Contributions of Medial Temporal Lobe and Striatal Memory Systems to Learning and Retrieving Overlapping Spatial Memories. *Cereb. Cortex*, *24*(7), 1906–1922. https://doi.org/10.1093/cercor/bht041

Brunec, I. K., Robin, J., Olsen, R. K., Moscovitch, M., & Barense, M. D. (2020). Integration and differentiation of hippocampal memory traces. *Neuroscience & Biobehavioral Reviews*, *118*(March), 196–208. https://doi.org/10.1016/j.neubiorev.2020.07.024

Buzsáki, G., & Moser, E. I. (2013). Memory, navigation and theta rhythm in the hippocampal-entorhinal system. *Nature Neuroscience*, *16*(2), 130–138. https://doi.org/10.1038/nn.3304

Buzsáki, G., & Tingley, D. (2018). Space and Time: The Hippocampus as a Sequence Generator. *Trends in Cognitive Sciences*, *22*(10), 853–869. https://doi.org/10.1016/j.tics.2018.07.006

Chanales, A. J. H., Dudukovic, N. M., Richter, F. R., & Kuhl, B. A. (2019). Interference between overlapping memories is predicted by neural states during learning. *Nature Communications*, *10*(1). https://doi.org/10.1038/s41467-019-13377-x

Chanales, A. J. H., Oza, A., Favila, S. E., & Kuhl, B. A. (2017). Overlap among Spatial Memories Triggers Repulsion of Hippocampal Representations Article Overlap among Spatial Memories Triggers Repulsion of Hippocampal Representations. *Current Biology*, *27*(15), 2307–2317. https://doi.org/10.1016/j.cub.2017.06.057

Chawla, M. K., Guzowski, J. F., Ramirez-Amaya, V., Lipa, P., Hoffman, K. L., Marriott, L. K., Worley, P. F., McNaughton, B. L., & Barnes, C. A. (2005). Sparse, environmentally selective expression of Arc RNA in the upper blade of the rodent fascia dentata by brief spatial experience. *Hippocampus*, *15*(5), 579–586. https://doi.org/10.1002/hipo.20091

Chung, A., Jou, C., Grau-Perales, A., Levy, E. R. J., Dvorak, D., Hussain, N., & Fenton, A. A. (2021). Cognitive control persistently enhances hippocampal information processing. *Nature*. https://doi.org/10.1038/s41586-021-04070-5

Clewett, D., & Davachi, L. (2017). The ebb and flow of experience determines the temporal structure of memory. *Current Opinion in Behavioral Sciences*, *17*, 186–193. https://doi.org/10.1016/j.cobeha.2017.08.013

Clewett, D., DuBrow, S., & Davachi, L. (2019). Transcending time in the brain: How event memories are constructed from experience. *Hippocampus*, *29*(3), 162–183. https://doi.org/10.1002/hipo.23074

Cohn-Sheehy, B. I., Delarazan, A. I., Reagh, Z. M., Barnett, A. J., Zacks, J. M., & Ranganath, C. (2021). The hippocampus constructs narrative memories across distant events. *Curr. Biol.*, *31*, 1–11. https://doi.org/10.1016/j.cub.2021.09.013

Collins, A. M., & Quillian, M. R. (1969). Retrieval time from semantic memory. *Journal of Verbal Learning and Verbal Behavior*, *8*, 240–247.

Copara, M. S., Hassan, A. S., Kyle, C. T., Libby, L. A., Ranganath, C., & Ekstrom, A. D. (2014). Complementary roles of human hippocampal subregions during retrieval of spatiotemporal context. *J Neurosci*, *34*(20), 6834–6842. https://doi.org/10.1523/JNEUROSCI.5341-13.2014

Cordes, D., Haughton, V. M., Arfanakis, K., Carew, J. D., Turski, P. A., Moritz, C. H., Quigley, M. A., & Elizabeth Meyerand, A. M. (2001). Frequencies Contributing to Functional Connectivity in the Cerebral Cortex in "'Resting-state'" Data. *ANJR Am J Neuroradiol*, *22*, 1326–1333.

Danielson, N. B., Kaifosh, P., Zaremba, J. D., Lovett-Barron, M., Tsai, J., Denny, C. A., Balough, E. M., Goldberg, A. R., Drew, L. J., Hen, R., Losonczy, A., & Kheirbek, M. A. (2016). Distinct Contribution of Adult-Born Hippocampal Granule Cells to Context Encoding. *Neuron*, *90*(1), 101–112. https://doi.org/10.1016/j.neuron.2016.02.019

Davachi, L., & DuBrow, S. (2015). How the hippocampus preserves order: The role of prediction and context. *Trends in Cognitive Sciences*, *19*(2), 92–99. https://doi.org/10.1016/j.tics.2014.12.004

de Sousa, A. F., Chowdhury, A., & Silva, A. J. (2021). Dimensions and mechanisms of memory organization. *Neuron*, *109*(17), 2649–2662. https://doi.org/10.1016/j.neuron.2021.06.014

Deuker, L., Bellmund, J. L. S., Navarro Schröder, T., & Doeller, C. F. (2016). An event map of memory space in the hippocampus. *Elife*, *5*, e16534. https://doi.org/10.7554/eLife.16534

Dimsdale-Zucker, H. R., & Ranganath, C. (2018). Representational Similarity Analyses: A Practical Guide for Functional MRI Applications. In D. Manahan-Vaughan (Ed.), *Handbook of Behavioral Neuroscience* (Vol. 28, pp. 509–525). https://doi.org/10.1016/B978-0-12-812028-6.00027-6

Dimsdale-Zucker, H. R., Ritchey, M., Ekstrom, A. D., Yonelinas, A. P., & Ranganath, C. (2018). CA1 and CA3 differentially support spontaneous retrieval of episodic contexts within human hippocampal subfields. *Nature Communications*, *9*(294). https://doi.org/10.1038/s41467-017-02752-1

DuBrow, S., & Davachi, L. (2013). The influence of context boundaries on memory for the sequential order of events. *Journal of Experimental Psychology: General*, *142*(4), 1277–1286. https://doi.org/10.1037/a0034024

DuBrow, S., & Davachi, L. (2014). Temporal Memory Is Shaped by Encoding Stability and Intervening Item Reactivation. *Journal of Neuroscience*, *34*(42), 13998–14005. https://doi.org/10.1523/jneurosci.2535-14.2014

DuBrow, S., & Davachi, L. (2017). Commentary: Distinct neural mechanisms for remembering when an event occurred. *Front. Psychol.*, *8*, 189. https://doi.org/10.3389/fpsyg.2017.00189

Duncan, K., Ketz, N., Inati, S. J., & Davachi, L. (2012). Evidence for area CA1 as a match/mismatch detector: A high-resolution fMRI study of the human hippocampus. *Hippocampus*, *22*(3), 389–398. https://doi.org/10.1002/hipo.20933

Duncan, K., & Schlichting, M. L. (2018). Hippocampal representations as a function of time, subregion, and brain state. *Neurobiology of Learning and Memory*, *153*, 40–56.

Duncan, K., Tompary, A., & Davachi, L. (2014). Associative encoding and retrieval are predicted by functional connectivity in distinct hippocampal area CA1 pathways. *Journal of Neuroscience, 34*(34), 11188–11198. https://doi.org/10.1523/JNEUROSCI.0521-14.2014

Eichenbaum, H. (2004). Hippocampus: Cognitive Processes and Neural Representations that Underlie Declarative Memory. *Neuron*, *44*(2), 109–120. https://doi.org/10.1016/j.neuron.2004.08.028

Eichenbaum, H. (2014). Time cells in the hippocampus: A new dimension for mapping memories. *Nature Reviews Neuroscience*, *15*(11), 732–744. https://doi.org/10.1038/nrn3827

Eichenbaum, H. (2017). On the Integration of Space, Time, and Memory. *Neuron*, *95*(5), 1007–1018. https://doi.org/10.1016/j.neuron.2017.06.036

Ezzyat, Y., & Davachi, L. (2011). What constitutes an episode in episodic memory? *Psychological Science*, *22*(2), 243–252. https://doi.org/10.1177/0956797610393742

Ezzyat, Y., & Davachi, L. (2014). Similarity breeds proximity: Pattern similarity within and across contexts is related to later mnemonic judgments of temporal proximity. *Neuron*, *81*(5), 1179–1189. https://doi.org/10.1016/j.neuron.2014.01.042

Favila, S. E., Chanales, A. J. H., & Kuhl, B. A. (2016). Experience-dependent hippocampal pattern differentiation prevents interference during subsequent learning. *Nature Communications*, *6*, 1–10. https://doi.org/10.1038/ncomms11066

Franklin, N. T., Norman, K. A., Ranganath, C., Zacks, J. M., & Gershman, S. J. (2020). Structured Event Memory: A neuro-symbolic model of event cognition. *Psychol. Rev.*, *127*(3), 327–361. https://doi.org/10.1037/rev0000177

Garvert, M. M., Dolan, R. J., & Behrens, T. E. J. (2017). A map of abstract relational knowledge in the human hippocampal–entorhinal cortex. *Elife*, *6*, e17086. https://doi.org/10.7554/eLife.17086

Gernsbacher, M. A. (1985). Surface information loss in comprehension. *Cognitive Psychology*, *17*(3), 324–363. https://doi.org/10.1016/0010-0285(85)90012-X

Ghosh, V. E., & Gilboa, A. (2014). What is a memory schema? A historical perspective on current neuroscience literature. *Neuropsychologia*, *53*(1), 104–114. https://doi.org/10.1016/j.neuropsychologia.2013.11.010

Gilboa, A., & Moscovitch, M. (2021). No consolidation without representation: Correspondence between neural and psychological representations in recent and remote memory. *Neuron*, *109*(14), 2239–2255. https://doi.org/10.1016/j.neuron.2021.04.025

Grande, X., Berron, D., Horner, A. J., Bisby, J. A., Düzel, E., & Burgess, N. (2019). Holistic Recollection via Pattern Completion Involves Hippocampal Subfield CA3. *Journal of Neuroscience*, *39*(41), 8100–8111. https://doi.org/10.1523/JNEUROSCI.0722-19.2019

Griffiths, B. J., & Fuentemilla, L. (2020). Event conjunction: How the hippocampus integrates episodic memories across event boundaries. *Hippocampus*, *30*(2), 162–171. https://doi.org/10.1002/hipo.23161

Hainmueller, T., & Bartos, M. (2020). Dentate gyrus circuits for encoding, retrieval and discrimination of episodic memories. *Nature Reviews Neuroscience*. https://doi.org/10.1038/s41583-019-0260-z

Hard, B. M., Tversky, B., & Lang, D. S. (2006). Making sense of abstract events: Building event schemas. *Memory and Cognition*, *34*(6), 1221–1235. https://doi.org/10.3758/BF03193267

Hasselmo, M. E., & Eichenbaum, H. (2005). Hippocampal mechanisms for the context-dependent retrieval of episodes. *Neural Networks*, *18*(9), 1172–1190. https://doi.org/10.1016/j.neunet.2005.08.007

Hasselmo, M. E., & Wyble, B. P. (1997). Free recall and recognition in a network model of the hippocampus: Simulating effects of scopolamine on human memory function. *Behavioural Brain Research*, *89*(1–2), 1–34. https://doi.org/10.1016/S0166-4328(97)00048-X

Heusser, A. C., Ezzyat, Y., Shiff, I., & Davachi, L. (2018). Perceptual boundaries cause mnemonic trade-offs between local boundary processing and across-trial associative binding.

Journal of Experimental Psychology: Learning Memory and Cognition, *44*(7), 1075–1090. https://doi.org/10.1037/xlm0000503

Heusser, A. C., Poeppel, D., Ezzyat, Y., & Davachi, L. (2016). Episodic sequence memory is supported by a theta-gamma phase code. *Nature Neuroscience*, *19*(10), 1374–1380. https://doi.org/10.1038/nn.4374

Hindy, N. C., Ng, F. Y., & Turk-Browne, N. B. (2016). Linking pattern completion in the hippocampus to predictive coding in visual cortex. *Nature Neuroscience*, *19*(5), 665–667. https://doi.org/10.1038/nn.4284

Horner, A. J., Bisby, J. A., Bush, D., Lin, W.-J., & Burgess, N. (2015). Evidence for holistic episodic recollection via hippocampal pattern completion. *Nature Communications*, *6*(May), 7462. https://doi.org/10.1038/ncomms8462

Horner, A. J., & Burgess, N. (2014). Pattern completion in multielement event engrams. *Current Biology*, *24*(9), 988–992. https://doi.org/10.1016/j.cub.2014.03.012

Horner, A. J., & Doeller, C. F. (2017). Plasticity of hippocampal memories in humans. *Current Opinion in Neurobiology*, *43*, 102–109. https://doi.org/10.1016/j.conb.2017.02.004

Howard, M. W., Fotedar, M. S., Datey, A. V., & Hasselmo, M. E. (2005). The temporal context model in spatial navigation and relational learning: Toward a common explanation of medial temporal lobe function across domains. *Psychological Review*, *112*(1), 75–116. https://doi.org/10.1037/0033-295X.112.1.75

Howard, M. W., & Kahana, M. J. (2002). A distributed representation of temporal context. *Journal of Mathematical Psychology*, *46*(3), 269–299. https://doi.org/10.1006/jmps.2001.1388

Hsieh, L.-T., Gruber, M. J., Jenkins, L. J., & Ranganath, C. (2014). Hippocampal Activity Patterns Carry Information about Objects in Temporal Context. *Neuron*, *81*(5), 1165–1178. https://doi.org/10.1016/j.neuron.2014.01.015

Hulbert, J. C., & Norman, K. A. (2014). Neural differentiation tracks improved recall of competing memories following interleaved study and retrieval practice. *Cerebral Cortex*, *25*(10), 3994–4008. https://doi.org/10.1093/cercor/bhu284

Iglesias, J. E., Augustinack, J. C., Nguyen, K., Player, C. M., Player, A., Wright, M., Roy, N., Frosch, M. P., McKee, A. C., Wald, L. L., Fischl, B., & Van Leemput, K. (2015). A computational atlas of the hippocampal formation using ex vivo, ultra-high resolution MRI: Application to adaptive segmentation of in vivo MRI. *NeuroImage*, *115*, 117–137. https://doi.org/10.1016/j.neuroimage.2015.04.042

Jafarpour, A., Griffin, S., Lin, J. J., & Knight, R. T. (2019). Medial Orbitofrontal Cortex, Dorsolateral Prefrontal Cortex, and Hippocampus Differentially Represent the Event Saliency. *J. Cogn. Neurosci.*, *31*(6), 874–884. https://doi.org/10.1162/jocn_a_01392

Jenkins, L. J., & Ranganath, C. (2016). Distinct Neural Mechanisms for Remembering When an Event Occurred. *Hippocampus*, *26*, 554–559. https://doi.org/10.1002/hipo.22571

Jung, M. W., & McNaughton, B. L. (1993). Spatial selectivity of unit activity in the hippocampal granular layer. *Hippocampus*, *3*(2), 165–182. https://doi.org/10.1002/hipo.450030209

Kalm, K., Davis, M. H., & Norris, D. (2013). Individual Sequence Representations in the Medial Temporal Lobe. *Journal of Cognitive Neuroscience*, *25*(7), 1111–1121. https://doi.org/10.1162/jocn

Kesner, R. P. (2018). An analysis of dentate gyrus function (an update). *Behavioural Brain Research*, *354*, 84–91.

Kesner, R. P., & Rolls, E. T. (2015). A computational theory of hippocampal function, and tests of the theory: New developments. *Neuroscience and Biobehavioral Reviews*, *48*, 92–147. https://doi.org/10.1016/j.neubiorev.2014.11.009

Kim, G., Norman, K. A., & Turk-Browne, N. B. (2017). Neural differentiation of incorrectly predicted memories. *Journal of Neuroscience*, *37*(8), 2022–2031. https://doi.org/10.1523/JNEUROSCI.3272-16.2017

Kirwan, C. B., & Stark, C. E. L. (2007). Overcoming interference: An fMRI investigation of pattern separation in the medial temporal lobe. *Learn. Mem.*, *14*(9), 625–633. https://doi.org/10.1101/lm.663507

Kleiner, M., Brainard, D., Pelli, D., Ingling, A., Murray, R., & Broussard, C. (2007). What's new in Psychtoolbox-3? *Perception*, *36*(14).

Knierim, J. J., & Neunuebel, J. P. (2016). Tracking the flow of hippocampal computation: Pattern separation, pattern completion, and attractor dynamics. *Neurobiology of Learning and Memory*, *129*, 38–49. https://doi.org/10.1016/j.nlm.2015.10.008

Kok, P., & Turk-Browne, N. B. (2018). Associative prediction of visual shape in the hippocampus. *Journal of Neuroscience*, *38*(31), 6888–6899. https://doi.org/10.1523/JNEUROSCI.0163-18.2018

Koolschijn, R. S., Emir, U. E., Pantelides, A. C., Nili, H., Behrens, T. E. J., & Barron, H. C. (2019). The Hippocampus and Neocortical Inhibitory Engrams Protect against Memory Interference. *Neuron*, *101*(3), 528–541. https://doi.org/10.1016/j.neuron.2018.11.042

Kriegeskorte, N., Goebel, R., & Bandettini, P. (2006). Information-based functional brain mapping. *Proceedings of the National Academy of Sciences of the United States of America*, *103*(10), 3863–3868. https://doi.org/10.1073/pnas.0600244103

Kriegeskorte, N., Mur, M., & Bandettini, P. (2008). Representational similarity analysis—Connecting the branches of systems neuroscience. *Frontiers in Systems Neuroscience*, *2*, 1–28. https://doi.org/10.3389/neuro.06.004.2008

Kuhl, B. A., Bainbridge, W. A., & Chun, M. M. (2012). Neural Reactivation Reveals Mechanisms for Updating Memory. *Journal of Neuroscience*, *32*(10), 3453–3461. https://doi.org/10.1523/JNEUROSCI.5846-11.2012

Kuhl, B. A., & Chun, M. M. (2014). Successful Remembering Elicits Event-Specific Activity Patterns in Lateral Parietal Cortex. *Journal of Neuroscience*, *34*(23), 8051–8060. https://doi.org/10.1523/JNEUROSCI.4328-13.2014

Kyle, C. T., Smuda, D. N., Hassan, A. S., & Ekstrom, A. D. (2015). Roles of human hippocampal subfields in retrieval of spatial and temporal context. *Behavioural Brain Research*, *278*, 549–558. https://doi.org/10.1016/j.bbr.2014.10.034

Kyle, C. T., Stokes, J. D., Lieberman, J. S., Hassan, A. S., & Ekstrom, A. D. (2015). Successful retrieval of competing spatial environments in humans involves hippocampal pattern separation mechanisms. *ELife*, 1–19. https://doi.org/10.7554/eLife.10499

Lacy, J. W., Yassa, M. A., Stark, S. M., Muftuler, L. T., & Stark, C. E. L. (2011). Distinct pattern separation related transfer functions in human CA3/dentate and CA1 revealed using high-resolution fMRI and variable mnemonic similarity. *Learning & Memory*, *18*(1), 15–18. https://doi.org/10.1101/lm.1971111

Lee, I., Yoganarasimha, D., Rao, G., & Knierim, J. J. (2004). Comparison of population coherence of place cells in hippocampal subfields CA1 and CA3. *Nature*, *430*(6998), 456–459. https://doi.org/10.1038/nature02739

Leutgeb, J. K., Leutgeb, S., Moser, M.-B., & Moser, E. I. (2007). Pattern separation in the dentate gyrus and CA3 of the hippocampus. *Science*, *315*(5814), 961–966. https://doi.org/10.1126/science.1135801

Leutgeb, S., & Leutgeb, J. K. (2007). Pattern separation, pattern completion, and new neuronal codes within a continuous CA3 map. *Learning & Memory*, *14*(11), 745–757. https://doi.org/10.1101/lm.703907

Levy, W. B. (1996). A sequence predicting CA3 is a flexible associator that learns and uses context to solve hippocampal-like tasks. *Hippocampus*, *6*(6), 579–590. https://doi.org/10.1002/(SICI)1098-1063(1996)6:6<579::AID-HIPO3>3.0.CO;2-C

Liu, C., Ye, Z., Chen, C., Axmacher, N., & Xue, G. (2022). Hippocampal Representations of Event Structure and Temporal Context during Episodic Temporal Order Memory. *Cerebral Cortex*, *32*(7), 1520–1534. https://doi.org/10.1093/cercor/bhab304

Lo, S., & Andrews, S. (2015). *To transform or not to transform: Using generalized linear mixed models to analyse reaction time data*. *6*(August), 1–16. https://doi.org/10.3389/fpsyg.2015.01171

Lohnas, L. J., Polyn, S. M., & Kahana, M. J. (2015). *Expanding the Scope of Memory Search: Modeling Intralist and Interlist Effects in Free Recall*. *122*(2), 337–363.

Long, N. M., & Kahana, M. J. (2019). *Hippocampal contributions to serial-order memory*. *July 2018*, 252–259. https://doi.org/10.1002/hipo.23025

Lositsky, O., Chen, J., Toker, D., Honey, C. J., Shvartsman, M., Poppenk, J. L., Hasson, U., & Norman, K. A. (2016). Neural pattern change during encoding of a narrative predicts retrospective duration estimates. *ELife*, *5*(NOVEMBER2016), 1–40. https://doi.org/10.7554/eLife.16070

Lüdecke, D. (2020). *sjstats: Statistical Functions for Regression Models (Version 0.18.0)*.

Mack, M. L., Love, B. C., & Preston, A. R. (2018). Building concepts one episode at a time: The hippocampus and concept formation. *Neuroscience Letters*, *680*, 31–38. https://doi.org/10.1016/j.neulet.2017.07.061

Madar, A. D., Ewell, L. A., & Jones, M. V. (2019). Temporal pattern separation in hippocampal neurons through multiplexed neural codes. *PLoS Comput. Biol.*, *15*(4), e1006932. https://doi.org/10.1371/journal.pcbi.1006932

Manns, J. R., Howard, M. W., & Eichenbaum, H. (2007). Gradual Changes in Hippocampal Activity Support Remembering the Order of Events. *Neuron*, *56*(3), 530–540. https://doi.org/10.1016/j.neuron.2007.08.017

Marr, D. (1971). Simple memory: A theory for archicortex. *Philosophical Transactions of the Royal Society of London. Series B, Biological Sciences*, *262*(841), 23–81.

Maurer, A. P., & Nadel, L. (2021). The Continuity of Context: A Role for the Hippocampus. *Trends in Cognitive Sciences*, *25*(3), 187–199. https://doi.org/10.1016/j.tics.2020.12.007

McKenzie, S., Frank, A. J., Kinsky, N. R., Porter, B., Rivière, P. D., & Eichenbaum, H. (2014). Hippocampal representation of related and opposing memories develop within distinct, hierarchically organized neural schemas. *Neuron*, *83*(1), 202–215. https://doi.org/10.1016/j.neuron.2014.05.019

Mizrak, E., Bouffard, N. R., Libby, L. A., Boorman, E. D., & Ranganath, C. (2021). The hippocampus and orbitofrontal cortex jointly represent task structure during memory-guided decision making. *Cell Rep.*, *37*(9), 110065. https://doi.org/10.1016/j.celrep.2021.110065

Molitor, R. J., Sherrill, K. R., Morton, N. W., Miller, A. A., & Preston, A. R. (2021). Memory Reactivation during Learning Simultaneously Promotes Dentate Gyrus/CA2,3 Pattern Differentiation and CA1 Memory Integration. *Journal of Neuroscience*, *41*(4), 726–738. https://doi.org/10.1523/JNEUROSCI.0394-20.2020

Morris, A. M., Curtis, B. J., Churchwell, J. C., Maasberg, D. W., & Kesner, R. P. (2013). Temporal associations for spatial events: The role of the dentate gyrus. *Behavioural Brain Research*, *256*, 250–256. https://doi.org/10.1016/j.bbr.2013.08.021

Morton, N. W., Sherrill, K. R., & Preston, A. R. (2017). Memory integration constructs maps of space, time, and concepts. *Curr Opin Behav Sci*, *17*, 161–168. https://doi.org/10.1016/j.cobeha.2017.08.007

Moscovitch, M., Cabeza, R., Winocur, G., & Nadel, L. (2016). Episodic memory and beyond: The hippocampus and neocortex in transformation. *Annual Review of Psychology*, *67*(1), 105–134. https://doi.org/10.1146/annurev-psych-113011-143733

Mumford, J. A., Davis, T., & Poldrack, R. A. (2014). The impact of study design on pattern estimation for single-trial multivariate pattern analysis. *NeuroImage*, *103*, 130–138. https://doi.org/10.1016/j.neuroimage.2014.09.026

Murphy, G. L. (2004). *The big book of concepts*. MIT press.

Myers, C. E., & Scharfman, H. E. (2011). Pattern separation in the dentate gyrus: A role for the CA3 backprojection. *Hippocampus*, *21*(11), 1190–1215. https://doi.org/10.1002/hipo.20828

Nakazawa, K. (2017). Dentate Mossy Cell and Pattern Separation. *Neuron*, *93*(3), 465–467. https://doi.org/10.1016/j.neuron.2017.01.021

Neunuebel, J. P., & Knierim, J. J. (2014). CA3 retrieves coherent representations from degraded input: Direct evidence for CA3 pattern completion and dentate gyrus pattern separation. *Neuron*, *81*(2), 416–427. https://doi.org/10.1016/j.neuron.2013.11.017

Newman, E. L., & Hasselmo, M. E. (2014). CA3 sees the big picture while dentate gyrus splits hairs. *Neuron*, *81*(2), 226–228. https://doi.org/10.1016/j.neuron.2014.01.004

Newton, A. T., Morgan, V. L., Rogers, B. P., & Gore, J. C. (2011). Modulation of steady state functional connectivity in the default mode and working memory networks by cognitive load: Modulation of Connectivity. *Human Brain Mapping*, *32*(10), 1649–1659. https://doi.org/10.1002/hbm.21138

Nieh, E. H., Schottdorf, M., Freeman, N. W., Low, R. J., Lewallen, S., Koay, S. A., Pinto, L., Gauthier, J. L., Brody, C. D., & Tank, D. W. (2021). Geometry of abstract learned knowledge in the hippocampus. *Nature*, *595*(7865), 80–84. https://doi.org/10.1038/s41586-021-03652-7

Norman, K. A., Newman, E., Detre, G., & Polyn, S. (2006). How inhibitory oscillations can train neural networks and punish competitors. *Neural Computation*, *18*, 1577–1610. https://doi.org/10.1162/neco.2006.18.7.1577

Norman, K. A., & O'Reilly, R. C. (2003). Modeling hippocampal and neocortical contributions to recognition memory: A complementary-learning-systems approach. *Psychological Review*, *110*(4), 611–646. https://doi.org/10.1037/0033-295X.110.4.611

O'Keefe, J., & Dostrovsky, J. (1971). The hippocampus as a spatial map. Preliminary evidence from unit activity in the freely-moving rat. *Brain Research*, *34*(1), 171–175.

O'Keefe, J., & Nadel, L. (1978). *The Hippocampus as a Cognitive Map*. Oxford University Press.

O'Reilly, R. C., & McClelland, J. L. (1994). Hippocampal conjunctive encoding, storage, and recall: Avoiding a trade-off. *Hippocampus*, *4*(6), 661–682. https://doi.org/10.1002/hipo.450040605

Pastalkova, E., Itskov, V., Amarasingham, A., & Buzsáki, G. (2008). Internally Generated Cell Assembly Sequences in the Rat Hippocampus. *Science*, *321*(5894), 1322–1328.

Paz, R., Gelbard-Sagiv, H., Mukamel, R., Harel, M., Malach, R., & Fried, I. (2010). A neural substrate in the human hippocampus for linking successive events. *Proceedings of the National Academy of Sciences*, *107*(13), 6046–6051. https://doi.org/10.1073/pnas.0910834107

Pelli, D. G. (1997). The VideoToolbox software for visual psychophysics: Transforming numbers into movies. *Spatial Vision*, *10*, 437–442.

Pettijohn, K. A., & Radvansky, G. A. (2016). Narrative event boundaries, reading times, and expectation. *Memory & Cognition*, *44*(7), 1064–1075. https://doi.org/10.3758/s13421-016-0619-6

Polyn, S. M., Norman, K. A., & Kahana, M. J. (2009). A Context Maintenance and Retrieval Model of Organizational Processes in Free Recall. *Psychological Review*, *116*(1), 129–156. https://doi.org/10.1037/a0014420

R core team. (2018). *R: A language and environment for statistical computing. R Foundation for Statistical Computing, Vienna, Austria. Https://www.r-project.org/.*

Radvansky, G. A., & Zacks, J. M. (2017). Event boundaries in memory and cognition. *Current Opinion in Behavioral Sciences*, *17*, 133–140. https://doi.org/10.1016/j.cobeha.2017.08.006

Ranganath, C., & Hsieh, L.-T. (2016). The hippocampus: A special place for time. *Annals of the New York Academy of Sciences*, *1369*(1), 93–110. https://doi.org/10.1111/nyas.13043

Renoult, L., Irish, M., Moscovitch, M., & Rugg, M. D. (2019). From Knowing to Remembering: The Semantic – Episodic Distinction. *Trends in Cognitive Sciences*, *23*(12), 1041–1057. https://doi.org/10.1016/j.tics.2019.09.008

Ritvo, V. J. H., Turk-Browne, N. B., & Norman, K. A. (2019). Nonmonotonic Plasticity: How Memory Retrieval Drives Learning. *Trends Cogn. Sci.*, *23*(9), 726–742. https://doi.org/10.1016/j.tics.2019.06.007

Robin, J., & Moscovitch, M. (2017). Details, gist and schema: Hippocampal–neocortical interactions underlying recent and remote episodic and spatial memory. *Current Opinion in Behavioral Sciences*, *17*, 114–123. https://doi.org/10.1016/j.cobeha.2017.07.016

Rolls, E. T. (2016). Pattern separation, completion, and categorisation in the hippocampus and neocortex. *Neurobiology of Learning and Memory*, *129*, 4–28. https://doi.org/10.1016/j.nlm.2015.07.008

Rueckemann, J. W., Sosa, M., Giocomo, L. M., & Buffalo, E. A. (2021). The grid code for ordered experience. *Nat. Rev. Neurosci.* https://doi.org/10.1038/s41583-021-00499-9

Schank, R., & Abelson, R. (1977). Scripts. In *Scripts Plans Goals and Understanding: An inquiry into human knowledge structures* (pp. 36–68). https://doi.org/10.1515/9789048536825-005

Schapiro, A. C., Kustner, L. V., & Turk-Browne, N. B. (2012). Shaping of object representations in the human medial temporal lobe based on temporal regularities. *Current Biology*, *22*(17), 1622–1627. https://doi.org/10.1016/j.cub.2012.06.056

Schapiro, A. C., Turk-Browne, N. B., Norman, K. A., & Botvinick, M. M. (2016). Statistical learning of temporal community structure in the hippocampus. *Hippocampus*, *26*(1), 3–8. https://doi.org/10.1002/hipo.22523

Scharfman, H. E. (2007). The CA3 “backprojection” to the dentate gyrus. In *Progress in Brain Research* (Vol. 163, pp. 627–637). Elsevier. https://doi.org/10.1016/S0079-6123(07)63034-9

Schendan, H. E., Searl, M. M., Melrose, R. J., & Stern, C. E. (2003). An FMRI study of the role of the medial temporal lobe in implicit and explicit sequence learning. *Neuron*, *37*(6), 1013–1025. https://doi.org/10.1016/s0896-6273(03)00123-5

Schlichting, M. L., Mumford, J. A., & Preston, A. R. (2015). Learning-related representational changes reveal dissociable integration and separation signatures in the hippocampus

and prefrontal cortex. *Nature Communications*, *6*(1), 1–10. https://doi.org/10.1038/ncomms9151

Shin, Y. S., & DuBrow, S. (2021). Structuring Memory Through Inference-Based Event Segmentation. *Top. Cogn. Sci.*, *13*(1), 106–127. https://doi.org/10.1111/tops.12505

Silva, M., Baldassano, C., & Fuentemilla, L. (2019). Rapid Memory Reactivation at Movie Event Boundaries Promotes Episodic Encoding. *Journal of Neuroscience*, *39*(43), 8538–8548. https://doi.org/10.1523/JNEUROSCI.0360-19.2019

Sols, I., DuBrow, S., Davachi, L., & Fuentemilla, L. (2017). Event Boundaries Trigger Rapid Memory Reinstatement of the Prior Events to Promote Their Representation in Long-Term Memory. *Current Biology*, *27*(22), 3499-3504.e4. https://doi.org/10.1016/j.cub.2017.09.057

Stark, C. E. L., & Squire, L. R. (2001). When zero is not zero: The problem of ambiguous baseline conditions in fMRI. *Proceedings of the National Academy of Sciences of the United States of America*, *98*(22), 12760–12765. https://doi.org/10.1073/pnas.221462998

Stokes, J., Kyle, C., & Ekstrom, A. D. (2015). Complementary Roles of Human Hippocampal Subfields in Differentiation and Integration of Spatial Context. *Journal of Cognitive Neuroscience*, *27*(3), 546–559. https://doi.org/10.1162/jocn

Sugar, J., & Moser, M. B. (2019). Episodic memory: Neuronal codes for what, where, and when. *Hippocampus*, *29*(12), 1190–1205. https://doi.org/10.1002/hipo.23132

Swallow, K. M., Zacks, J. M., & Abrams, R. A. (2009). Event Boundaries in Perception Affect Memory Encoding and Updating. *Journal of Experimental Psychology. General*, *138*(2), 236–257. https://doi.org/10.1109/TMI.2012.2196707.Separate

Tambini, A., & Davachi, L. (2013). Persistence of hippocampal multivoxel patterns into postencoding rest is related to memory. *Proc. Natl. Acad. Sci. U. S. A.*, *110*(48), 19591–19596. https://doi.org/10.1073/pnas.1308499110

Thavabalasingam, S., Neil, E. B. O., & Lee, A. C. H. (2018). Multivoxel pattern similarity suggests the integration of temporal duration in hippocampal event sequence representations. *NeuroImage*, *178*, 136–146. https://doi.org/10.1016/j.neuroimage.2018.05.036

Thavabalasingam, S., O'Neil, E. B., Tay, J., Nestor, A., & Lee, A. C. H. (2019). Evidence for the incorporation of temporal duration information in human hippocampal long-term memory sequence representations. *Proceedings of the National Academy of Sciences of the United States of America*, *116*(13), 6407–6414. https://doi.org/10.1073/pnas.1819993116

Theves, S., Neville, D., Fernández, G., & Doeller, C. F. (2021). Learning and Representation of Hierarchical Concepts in Hippocampus and Prefrontal Cortex. *Journal of Neuroscience,* https://doi.org/10.1523/JNEUROSCI.0657-21.2021

Tompary, A., & Davachi, L. (2017). Consolidation Promotes the Emergence of Representational Overlap in the Hippocampus and Medial Prefrontal Cortex. *Neuron*, *96*(1), 228–241. https://doi.org/10.1016/j.neuron.2017.09.005

Tompary, A., Duncan, K., & Davachi, L. (2015). Consolidation of Associative and Item Memory Is Related to Post-Encoding Functional Connectivity between the Ventral Tegmental Area and Different Medial Temporal Lobe Subregions during an Unrelated Task. *Journal of Neuroscience*, *35*(19), 7326–7331. https://doi.org/10.1523/JNEUROSCI.4816-14.2015

Tompary, A., Duncan, K., & Davachi, L. (2016). High-resolution investigation of memory-specific reinstatement in the hippocampus and perirhinal cortex. *Hippocampus*, *26*(8), 995–1007. https://doi.org/10.1002/hipo.22582

Treves, A., & Rolls, E. T. (1994). Computational Analysis of the role of hippocampus in memory. *Hippocampus*, *4*(3), 374–391.

Tulving, E. (1972). Episodic and semantic memory. In *Organization of memory* (Vol. 1, pp. 381–403). https://doi.org/10.1017/S0140525X00047257

Umbach, G., Kantak, P., Jacobs, J., Kahana, M., Pfeiffer, B. E., Sperling, M., & Lega, B. (2020). Time cells in the human hippocampus and entorhinal cortex support episodic memory. *Proc. Natl. Acad. Sci. U. S. A.*, *117*(45), 28463–28474. https://doi.org/10.1073/pnas.2013250117

Vazdarjanova, A., & Guzowski, J. F. (2004). Differences in hippocampal neuronal population responses to modifications of an environmental context: Evidence for distinct, yet complementary, functions of CA3 and CA1 ensembles. *Journal of Neuroscience, 24*(29), 6489–6496. https://doi.org/10.1523/JNEUROSCI.0350-04.2004

Wanjia, G., Favila, S. E., Kim, G., Molitor, R. J., & Kuhl, B. A. (2021). Abrupt hippocampal remapping signals resolution of memory interference. *Nat. Commun.*, *12*(1), 1–11. https://doi.org/10.1038/s41467-021-25126-0

Wisse, L. E. M., Daugherty, A. M., Olsen, R. K., Berron, D., Carr, V. A., Stark, C. E. L., Amaral, R. S. C., Amunts, K., Augustinack, J. C., Bender, A. R., Bernstein, J. D., Boccardi, M., Bocchetta, M., Burggren, A., Chakravarty, M. M., Chupin, M., Ekstrom, A., de Flores, R., Insausti, R., … la Joie, R. (2017). A harmonized segmentation protocol for hippocampal and

parahippocampal subregions: Why do we need one and what are the key goals? *Hippocampus*, *27*(1), 3–11. https://doi.org/10.1002/hipo.22671

Yassa, M. A., & Stark, C. E. L. (2011). Pattern separation in the hippocampus. *Trends in Neurosciences*, *34*(10), 515–525. https://doi.org/10.1016/j.tins.2011.06.006

Zacks, J. M. (2020). Event Perception and Memory. *Annual Review of Psychology*, *71*(1), 165–191. https://doi.org/10.1146/annurev-psych-010419-051101

Zacks, J. M., Kurby, C. A., Eisenberg, M. L., & Haroutunian, N. (2011). Prediction error associated with the perceptual segmentation of naturalistic events. *J. Cogn. Neurosci.*, *23*(12), 4057–4066. https://doi.org/10.1162/jocn_a_00078

Zacks, J. M., Speer, N. K., Swallow, K. M., Braver, T. S., & Reynolds, J. R. (2007). Event Perception: A Mind-Brain Perspective. *Psychological Bulletin*, *133*(2), 273–293. https://doi.org/10.1037/0033-2909.133.2.273

Zheng, J., Schjetnan, A. G. P., Yebra, M., Gomes, B. A., Mosher, C. P., Kalia, S. K., Valiante, T. A., Mamelak, A. N., Kreiman, G., & Rutishauser, U. (2022). Neurons detect cognitive boundaries to structure episodic memories in humans. *Nature Neuroscience*, *25*(3), 358–368. https://doi.org/10.1038/s41593-022-01020-w

Zheng, L., Gao, Z., McAvan, A. S., Isham, E. A., & Ekstrom, A. D. (2021). Partially overlapping spatial environments trigger reinstatement in hippocampus and schema representations in prefrontal cortex. *Nat. Commun.*, *12*(1), 6231. https://doi.org/10.1038/s41467-021-26560-w

Zwaan, R. A. (1996). Processing narrative time shifts. *Journal of Experimental Psychology: Learning, Memory, and Cognition*, *22*(5), 1196–1207. https://doi.org/10.1037/0278-7393.22.5.1196

Zwaan, R. A., Magliano, J. P., & Graesser, A. C. (1995). Dimensions of Situation Model Construction in Narrative Comprehension. *Journal of Experimental Psychology: Learning, Memory, and Cognition*, *21*(2), 386–397. https://doi.org/10.1037/0278-7393.21.2.386